Coastal Overwash: Processes and Modelling

Donnelly, Chantal

2008

**WATER RESOURCES ENGINEERING, FACULTY OF ENGINEERING,
LUND UNIVERSITY**

Doctoral Thesis

COASTAL OVERWASH:

PROCESSES AND MODELLING

By Chantal Donnelly

February 2008

Water Resources Engineering
Department of Building & Environmental engineering
Faculty of Engineering
Lund University
SE-221 00 Lund, Sweden.

Water Resources Engineering
Report LUTVDG/(TVVR-1043) (2007)
ISBN 978-91-628-7347-9
ISSN: 1101-9824
Report No. 1043
Printed in Sweden by Media-Tryck, Lund 2008

ACKNOWLEDGEMENTS

There are a few people I would like to acknowledge and thank for their help over the course of my doctorate education. First of all I would like to thank my supervisors, Professors Magnus Larson and Hans Hanson. I would like to thank Magnus, not only for his excellent advice, ideas and reviews, but also for his skill in guiding me along the way from research student to researcher with alot of freedom to develop my own direction and ideas. I would like to thank Hans for his continued interest in my professional development and contact network, and also for his helpful advice, ideas, and reviews over the last four years. I would also like to thank you both for giving me the opportunity to come to Lund for these studies.

My co-supervisor, Dr. Nicholas Kraus at the U.S. Army Engineering Research Development Center, is to be thanked for his invaluable help in acquiring data, developing my personal network, and getting me started with my first articles on overwash. Nick has given me an excellent network of colleagues in the field, given me the opportunity to conduct unique new laboratory experiments and maintained a continued interested in my progress, so thanks.

I would also like to thank Ty Wamsley, William Seaburgh, Hugh Acuff, Glenn Myrick, and Ken Connell, for their assistance with the laboratory experiments, Li Erikson for showing me the ropes at TVRL and for helping get started with digital image analysis, Don Stauble for his invaluable personal observations of real overwash on Assateague Island in the late 1970's and willingness to drag out 30 year old data and pictures, and Ana Matias for sharing her field data, field experiences and for an interesting collaboration on the last article. All those who have contributed data are too numerous to list here, but they are thanked in each of the individual articles. Thanks for taking the time to dig up old data and share it with me.

I would also like to thank the teachers from my undergraduate years: Hubert Chanson for fostering an interest in hydraulics and encouraging me to take it further, and Peter Nielsen for his encouragement and for introducing me to my supervisors in Sweden.

I would also like to thank my friends and colleagues at TVRL, for welcoming me here, patiently enduring my first attempts to speak Swedish, the fika and lunch discussions, technical help when needed and the fun 'after-work' nights. Thanks to all my family who always encouraged an interest in science, to my Dad who always answered the aubergine question, my Grandpa John who encouraged knowledge with coolmints, and to you all for accepting my choice to live on the other side of the world. Thanks to Oskar's family for making me a part of yours, and finally thanks to Oskar for putting up with me over the last four years.

Finally, I would like to thank the U.S. Army Corps of Engineers Coastal Inlets Research Program (CIRP) and the E.U. FLOODSITE project for financial support.

ABSTRACT

Overwash is the flow of water and sediment over the crest of a beach system when the runup level of waves or the water level, often enhanced by storm surge, exceeds the local beach or dune crest height. The impacts of overwash on coastal barriers or low lying mainland coasts are striking. Overwash may cause deposition of sand on and landward of the beach crest, large fan shaped deposits on back barriers, large sheet like deposits over an entire barrier, sand deposition into back barrier waterways, or may even lead to breaching of coastal barriers. It would therefore be highly useful to be able to predict the occurrence of overwash events and the magnitude and shape of the washover deposited during them. Although a number of studies describing overwash and washover deposits have been published, there remains a large scope to describe overwash processes, overwash hydrodynamics and to develop models for predicting the magnitude and shape of washover deposits on the back barrier.

The objective of this study was to improve the capability to predict sediment transport caused by overwash, and hence the resulting topographic changes. The sediment transported by overwash is a function of the overwash hydrodynamics, and the overwash hydrodynamics are affected by a number of different, interacting processes. One of the main tasks for this study was therefore to identify and describe both the forcing and back barrier processes that affect overwashing flow. Overwash was shown to occur due to both wave runup overtopping the beach crest and surge levels exceeding the beach crest height. On the back barrier, overwash hydrodynamics and sediment transport were shown to be affected by the back barrier water level, friction, infiltration, lateral spreading and anthropogenic influences.

New, mid-scale laboratory experiments of runup overwash were conducted to gain an understanding of back barrier flow hydrodynamics. The laboratory data were supplemented with published field data to derive relationships to estimate overtopping depths and wave front velocities on the beach crest and back barrier. Additionally, three different types of overwash model were developed. The first, a parametric model, uses simple, readily available data to predict the type of cross-shore morphodynamic change expected for a given incipient barrier profile and maximum storm characteristics. Secondly, an analytical model was derived to calculate order-of-magnitude beach face retreat and overwash volumes for schematised incipient beach profiles. Finally, a numerical model was developed to calculate in more detail the barrier profile change resulting from an overwash event. This model uses incipient beach profiles and a time-series of storm characteristics to calculate the beach profile change. All three models were calibrated, validated and verified against a large, new data set of pre- and post-storm beach profiles measured where overwash had occurred and show promising results for predicting beach profile change.

APPENDED PAPERS

This thesis is submitted with the support of the following papers which will be referred to by their numerals in the body of the text.

I. Donnelly, C., Kraus, N.C., and Larson, M. 2006. *State Of Knowledge on Measurement and Modeling of Coastal Overwash*. Journal of Coastal Research. 22 (4), 965-991.

II. Donnelly, C. 2007. *Morphology Change by Overwash: Establishing and Evaluating Predictors*. Journal of Coastal Research. SI 50, 520-526.

III. Larson, M.L., Donnelly, C., Jimenez, J., Hanson, H. (submitted). *Analytical model of beach erosion and overwash during storms*. Submitted to: Proceedings of ICE Maritime Engineering.

IV. Donnelly, C., Hanson, H. and Larson, M. (submitted). *A numerical model of coastal overwash.* Submitted to: Proceedings of ICE Maritime Engineering.

V. Donnelly, C., and Larson, M. (submitted). *Hydrodynamics of Runup Overwash.* Submitted to: Coastal Engineering

VI. Donnelly, C., Matias, A., and Chen, Q. (submitted). *Back Barrier Processes during Overwash.* Submitted to: Marine Geology

Other publications by the author related to the thesis and referred to in the thesis (selected on a competitive basis and edited):

- Donnelly, C., Ranasinghe, R., and Larson, M. 2006. *Numerical Modelling of Beach Profile Change caused by Overwash.* Proceedings Coastal Dynamics ’05. CD-ROM, ASCE, 14pp.

- Donnelly, C., Wamsley, T.V., Kraus, N.C., Larson, M., and Hanson, H. 2006. *Morphologic classification of coastal overwash*. Proceedings 30th International Conference on Coastal Engineering. ASCE, pp.2805-2817.

- Donnelly, C., and Sallenger, A. H. Jnr. 2007. *Characterisation and Modelling of Washover Fans*. Proceedings Coastal Sediments. ‘07, ASCE, pp. 2061-2073.

- Nguyen, X.T., Donnelly, C., and Larson, M. 2006. A new empirical formula for coastal overwash volume. *Proceedings Vietnam-Japan Estuary Workshop,* Water Resources University, Vietnam, 60-65. (Supervised Masters thesis)

ABBREVIATIONS AND SYMBOLS

The symbols and abbreviations listed here are consistent within the thesis summary. Alternative symbols used in the appended papers (I to VI) are also noted here.

A	Empirical constant relating overwash transport to offshore transport and runup level
B	Width of block of water moving on back barrier slope
B_D	Width of dune/beach crest 0.3 m below highest elevation recorded (Paper II), Initial width (width at crest) of block of water moving on back barrier slope (Paper IV)
C_d	Weir coefficient
C_{infilt}	Infiltration constant
C_{ls}	Lateral spreading constant
C_u	Bore front coefficient
D	Dune height
f_c	Friction coefficient on back barrier
F	Water level exceeding beach crest integrated over time
g	Acceleration due to gravity
h	Depth on back barrier
h_D	Water level exceeding the beach crest
h_o	Depth at SWL during maximum runup
H_c	Overtopping wave height
H_o	Significant deepwater wave height (maximum value during storm)
H_{ow}	Overwashing wave height
k_f	Friction coefficient on back barrier
K_B	Overwash transport coefficient (Paper IV), friction coefficient on back barrier (Paper V)
l	Length of block of water moving on back barrier slope
l_{Do}	Initial subaerial barrier width
l_o	Subaerial barrier width
MSL	Mean sea level
q_B	Cross-shore sediment transport over the beach crest
q_D	Cross-shore sediment transport rate over the beach crest
q_{DI}	Cross-shore sediment transport rate over the beach crest, inundation overwash
q_{DR}	Cross-shore sediment transport rate over the beach crest, runup overwash
q_o	Cross-shore sediment transport going offshore
R	Runup level (above SWL)
s	Distance along back barrier from beach crest
s_{ave}	Beach slope (between SWL and crest)

s_f	Front slope of dune
s_r	Rear slope of dune
S	Surge level above MSL (maximum surge level during storm, Paper II)
S_{bay}	Surge level above MSL on ocean side of barrier
S_{ocean}	Surge level above MSL on bay side of barrier
SWL	Still water level
T	Wave or swash period, in Paper II corresponding to max H_o.
t	Time
t_D	Duration of overtopping
t_{max}	Duration over which the water depth is increasing during a single overwashing wave, *i.e.*, the time between the arrival of the wave front and the time of peak water depth for that wave
t_s	Duration of overwash during a storm
t_{wetted}	Duration over which a single overwashing wave has a depth > 0 m at a fixed point in space
u_B	Overwash wave front velocity (on back barrier)
u_{crest}	Wave front velocity at crest, see also u_D (Paper IV)
V	Volume of sediment eroded from barrier
V_B	Volume of sediment transported landward as overwash
V_D	Dune volume (Paper II), Barrier volume (Paper III)
V_{Do}	Initial barrier volume
V_o	Volume of sediment mobilised by wave impact
$\dot{V}_{DI}$	Average flow rate over the beach crest (wave runup)
$\dot{V}_{DR}$	Average flow rate over the beach crest (inundation)
x_B	Cross-shore location of shoreward limit of barrier
x_{Bo}	Initial cross-shore location of shoreward limit of dune or barrier
x_c	Horizontal distance from SWL to the beach crest
x_o	Cross-shore location of seaward limit of barrier
x_{oo}	Initial cross-shore location of seaward limit of barrier
x_R	Horizontal projection of maximum runup from SWL
Z_D	Crest height above MSL, see also Y_c (Paper II), s (Paper III)
α	Infiltration rate constant
β_B	Back barrier slope, see also b (Paper IV)
β_{ave}	Beach slope (between SWL and crest)
β_f	Front slope of dune
β_r	Rear slope of dune
μ	Lateral spreading angle

CONTENTS

1 Introduction

1.1 Background

The number of people choosing to live on the coast is continuously increasing. Awareness of environmental issues on coasts, such as coastal ecosystem protection and preservation of natural coastal environments, is also increasing. Predicting how coastal regions are impacted by extreme storm events is therefore an increasingly important skill for coastal and even global societies. One of the most striking impacts of tropical and extra-tropical storms on coastal barriers and low lying mainland coasts is overwash. Overwash is the transport of sediment and water over the crest of a beach onto the mainland or back barrier behind. It occurs predominantly during extreme storms such as hurricanes and other severe storms, but non-storm overwash also occurs. It may cause, in order of increasing severity: a small build up of sediment on a dune crest; the deposition of a fan-shaped deposit spreading out on the back barrier behind a gap in a foredune; regional scale, unconstrained deposition of sand over a barrier island (sheetwash); the landward migration of a barrier, or even lead to the development of a breach through a barrier. All these processes are caused by water and sand overtopping the beach crest: overwash. The sediment deposited by overwash processes is called washover.

***Figure 1-1**. Overwash occurring over a low, flat barrier island on the Ria de Formosa, Portugal (photo courtesy of Ana Matias, University Algarve, Portugal)*

Overwash occurrence has predominantly been recorded on sandy barrier islands, but it has also been shown to occur on gravel and shingle beaches, on low-profile mainland coasts, and on lacustrine beaches. Worldwide, observations of overwash include occurrences in Australia, Canada, Denmark, Ireland, Portugal, Spain, Sweden, the U.K., U.S.A, on the Baltic Sea, on the Black sea and on the Great Lakes of Canada and the USA

There are many reasons to study overwash. There are geologic, ecologic and anthropogenic reasons for understanding overwash processes. The geologic role of overwash on coastal barriers is important. Overwash has been shown to be capable of causing the landward

migration of a barrier under a single storm event (Stone *et al.* 2004), and is thought to be an important mechanism in the response of transgressive barriers to sea-level rise (Dillon 1970, Kraft 1973).The ecologic role of overwash is likewise important. Washover has been shown to provide a platform for the development of new marsh (Godfrey and Godfrey 1974) and salt-resistant grasses, and, for example, has been shown to provide a vital ecosystem along the Atlantic and Gulf coasts of the USA to support an endangered species, the piping plover (*Charadrius meloduso*) (Kraus 2006).

The desire to live on coastal barriers leads to a number of anthropogenic and engineering reasons to study overwash. Overwash may cause flooding and sand intrusion into coastal communities. It may cause damage to coastal infrastructure such as shore parallel roads, and washover that reaches the back barrier bay may hinder navigation in the bay. Reduction of dune heights in association with overwash may reduce the future storm protection potential of the beach. The ability to predict the occurrence, location, and thickness of washover is therefore important for geologists, ecologists, coastal residents, coastal town planners, environmental planners, and engineers alike.

This thesis introduces new understanding of overwash processes and overwash hydrodynamics, developed for the purpose of modelling sediment transport and beach profile changes caused by overwash. In particular, morphologic changes and hydrodynamics at the crest are related to the forcing conditions, back barrier flow hydrodynamics and flow processes are defined, and simple methods for parametric, analytical and numerical prediction of cross-shore beach profile change by overwash are introduced. As part of this study, new field datasets were established consisting of: topographical pre- and post-storm data showing overwash occurrence with the associated hydrodynamic data for a wide variety of locations and storm conditions; a new laboratory study of overwash focusing on back barrier hydrodynamics; and the large amount of overwash observations published in overwash literature since the 1970's which are summarised in **Paper I**.

1.2 Objectives and Scope

The overall aim of this study was to improve the capability to predict sediment transport by overwash, and hence topographic changes caused by overwash. The focus of the study is restricted to changes on the beach crest, and the region behind the beach crest, for which we will use the term back barrier. The scope of the study was limited to sandy beach and barrier systems. Overwash is also an important process on gravel and shingle barriers (Carter and Orford 1981), and many of the same processes apply; however, the relative importance of different overwash processes on gravel and shingle barriers (for example, infiltration) will certainly be different.

From the point at which research on overwash was developed at the outset of this study, the following tasks were deemed necessary to achieve this aim:

1) Compile the existing literature on overwash in order to gain an overall understanding of overwash processes.

2) Collate existing and new overwash field and laboratory data.

3) Further develop the understanding of overwash processes.

4) Quantify overwash hydrodynamics.

5) Formulate mathematical models of overwash hydrodynamics and sediment transport, and hence predict cross-shore beach profile changes caused by overwash.

These tasks are addressed in a series of articles, appended to this thesis. The first research task is addressed in **Paper I**. This article summarised the state of knowledge of overwash measurements, processes and modelling at the time of writing, 2005. This state of knowledge is updated within this thesis summary. **Paper II** introduces a simple parametric method for determining the important factors that affect how a barrier cross-section responds to overwash, addressing task 3. These factors may then be used to qualitatively predict cross-shore profile response. Task 5 is addressed in **Papers III** and **IV**. Using the knowledge of overwash processes gained in the earlier work, a simple analytical model to predict profile response is presented in **Paper III.** Similarly, a numerical method to quantitatively predict cross-shore profile response to overwash was introduced in **Paper IV**. The progression of an article based thesis is not linear, and hence **Paper V** steps back to the fourth task, to quantify overwash hydrodynamics using both laboratory and field measurements. This paper also introduces new mathematical algorithms to predict overwash hydrodynamics. **Paper VI** again addresses overwash processes and hence task 3. Factors affecting the deposition of overwash on the back barrier are defined and their effects on back barrier flow inferred.

Herein, the summary of this thesis presents the contributions these papers have made to the understanding of overwash processes, hydrodynamics and modelling of overwash, defining the scope for each study, a brief description of the methodology and recapping the major results. A summary of all the data employed during the study is also presented, including a description of new mid-scale laboratory simulation of overwash conducted to support the study. New results arising from that study are also presented.

It is anticipated that the improved knowledge of overwash processes and hydrodynamics, and new approaches to overwash modelling developed within this study will lead to improved descriptions of physical processes in numerical modelling of topographical change caused by overwash. The improved description of overwash processes is also of use to geologists studying short- and long-term changes to barrier islands and using sedimentary records of overwash occurrences to identify storms.

1.3 Terminology

The term overwash has been applied by different researchers to describe different processes. One aim of this thesis was to encapsulate all the different processes which may be considered as overwash, and subsequently subcategorise the forcing and back barrier deposition processes that may lead to different sorts of washover deposits. Overwash was hence defined as the transport of sand and water over the crest of a beach onto the mainland or back barrier, deemed to occur if *either* wave runup level or water level exceeds the beach crest height (**Paper I**). This definition therefore captures morphologic changes ranging from accumulation overwash (deposition of sediment on the beach crest) to barrier disintegration (removal of sediment from the entire subaerial portion of a barrier), and all types of deposition on the back barrier. *It is important to have a definition that captures all processes occurring when a water, sediment mix overtops a beach crest.*

Here the term 'beach crest' is defined to mean the crest of the most seaward dune, or in the absence of dunes, the point on the beach from which there is a significant transition from a seaward to a landward trending slope. Because overwash extends the normal nearshore processes landward of the beach crest, some of the terminologies applied may be unfamiliar, unique or applied in a new way. The terminologies employed are therefore explained in Tables 1.1 and 1.2.

Table 1.1 Morphologic Terminology

Term	Description
Back barrier	The region of a barrier island, barrier spit, or mainland coast which is landward of the beach crest.
Back barrier bay	A body of water such as a lagoon or bay landward of a barrier spit or island.
Barriers islands	Elongated, shore-parallel, usually sandy features that parallel coasts in many places and are separated from the mainland by bodies of water of various sizes, and/or salt marshes, lagoons, mud, or sand flats, and tidal creeks. Here, the term may also be taken to refer to barrier spits.
Beach crest	The crest of the most seaward dune, or in the absence of dunes, the point on the beach from which there is a significant transition from a seaward to a landward trending slope.
Dune	A prominent feature at the landward end of the nearshore, formed by wind blown sand and/or long-term geological processes.
Foredune ridge	The ridge or line of dunes nearest to the ocean.
Rear dune ridge	Any ridge or line of dunes landward of the foredune ridge.
Swash zone	The swash zone is the region where the beach face is alternatively covered by the run-up of swash waves and exposed when the waves retreat. During runup overwash, the swash zone extends to the beach crest. It should be noted, however, that only a portion of the uprush returns seaward as backwash. During inundation overwash, the swash zone is not defined.
Washover	The sediment deposited by overwash.
Washover throat	A local depression in a dune ridge through which overwash has been focused.

Table 1.2 Hydrodynamic Terminology

Term	Description
Inundation overwash	Overwash occurring when the water level exceeds the beach crest level.
Overtopping	The flow of water over a beach or structure crest.
Overtopping wave height	The maximum water depth at the crest during a single overtopping wave event.
Overwash	The flow of water and sediment over the beach crest.
Overwash wave front velocity	The velocity of the wave front as it moves across the back barrier.
Overwashing wave height	The maximum water depth at a fixed point on the back barrier during a single overtopping wave event.
Runup height	When runup overwash occurs, this is defined as: the height above the still water level a wave would reach if the beach extended landwards above the beach crest at constant slope. This value includes wave setup. The runup height is not defined during inundation overwash.
Runup overwash	Overwash occurring when the runup level exceeds the beach crest level.
Swash front velocity	The velocity of the wave front as it moves through the swash zone.
Still Water level	The still water level including the effects of astronomical tide, storm surge and wind setup, but not wave setup.

2 Data Employed

A wide variety of data, both published and new, was employed during this study. Morphologic data includes pre- and post-storm surveyed cross-shore beach profiles from the field, pre- and post-storm topographic lidar data from the field, pre- and post-storm photography, real-time field measurements during overwash occurrences, and laboratory simulations of overwash. The latter two also provided both forcing data and hydrodynamic data relating to the resulting morphologies. Forcing data for the other data sets was retrieved from public data sets of tidal gauge measurements, wave buoy measurements, and wave hindcast results. Qualitative descriptions of observed overwash occurrences and recently deposited washover are also important sources of data that should be included in any complete description of the data used. Qualitative descriptions of overwash were acquired from the many published descriptions of overwash summarised in **Paper I**, and from personal communications with scientists present during overwash events (Stauble, pers.comm., and Matias, pers. comm.). Their experiments are described in Fisher and Stauble (1977) and Matias (2006).

2.1 Morphologic Data

Topographic elevations of a section of beach prior to and following a storm were compared to observe the morphological change caused by overwash. A large number of pre- and post-storm beach profiles were compiled both from published literature and from city, state, and consulting engineers, and beach protection authorities. Most of the available overwash profile sets are from the USA's Atlantic and Gulf coasts, with one data set from the south coast of Portugal. The American data sets include pre- and post-storm profiles from Metompkin Island (VI), Manasquan (NJ), Ocean City and Assateague Island (MD), the Outer Banks and Hatteras Island (NC), Folly, Garden City and North Myrtle Beaches (SC), Santa Rosa Island, Captiva and Sanibel Islands, Lovers Key, Martin County, St Lucie County and Fort Pierce (FL), and Chaland and Pelican Islands (LA). Details of the cross-shore beach profile sets are summarised in Donnelly *et al.* (2006). The median grain size of the beach sediment at the overwashed location was also collected.

The occurrence of overwash was identified if the post-storm profile indicated morphologic change on and behind the beach crest. These profiles were used to classify seven different cross-shore morphology change types resulting from overwash (Donnelly *et al.* 2006), and hence establish morphologic and hydrodynamic parameters for predicting the type of cross-shore profile response following overwash for given pre-storm profile and storm conditions (**Paper II**). They were also used to calibrate and verify analytical and numerical models for prediction of cross-shore profile change caused by overwash (**Paper III, Paper IV**).

High resolution, three-dimensional, pre-and post-storm topography collected by lidar (light detection and ranging) were also used to determine morphological changes caused by overwash. Airborne topographic lidar surveys allow the rapid collection of topographic data from large regions within a short period of time, making this a particularly suitable method for assessing the regional effects of storms on barrier systems (Sallenger *et al.* 2003). The lidar topography was used to study the three-dimensional morphologic changes caused by overwash, including the formation of washover fans (Donnelly and Sallenger 2007) and back barrier processes affecting the deposition of washover (**Paper VI**).

Real-time field measurements of beach profile change during and after overwash collected by Matias *et al.* (2006) were also employed in papers **II**, **III, V** and **VI**.

The laboratory data is discussed in section 2.3.

2.2 Forcing Data

Forcing data was collected for the aforementioned morphologic data sets to relate the observed morphologic changes to the storm forcing. The hydrodynamic forcing data important for overwash are water level, and wave height, period and direction.

Where available, wave characteristics were extracted from a nearby wave buoy. If the nearest wave buoy was positioned towards the edge of or off the continental shelf, hindcast wave data from the Wave Information Studies (WIS) model was used (http://frf.usace.army.mil/cgi-bin/wis/atl/atl_main.html). This was done to avoid having to calculate the dissipation of wave energy over the continental shelf. This was particularly important for **Paper III** because the model used to calculate the input conditions for overwash, SBEACH, does not take this into account (Larson and Kraus 1989, Wise et al. 1996). Water level data was extracted at the nearest gauge from the National Oceanic and Atmospheric Administration's (NOAA's) Tides Online historic data retrieval service. (http://tidesandcurrents.noaa.gov/station_retrieve.shtml?type=Historic+Tide+Data). The wave and water level data were available at hourly resolutions and were used to determine parameters significant to overwash such as water level and runup level (**Paper II**) and as input for numerical and analytical modelling of overwash (**Papers III and IV**). The time variation of storm surge levels, extracted from a storm surge model (Chen *et al.* submitted) and from field measurements of overwash (Matias 2006), was used to determine the effects of back barrier water levels on washover deposition (**Paper VI**).

2.3 Laboratory Data

A series of new, mid-scale experiments was conducted in a 2-dimensional wave flume at the U.S. Army Corps of Engineers Coastal Hydraulics Laboratory in Vicksburg, MS. The experiment series consisted of three different experiments, the first two of which relate to this thesis. Experiment 1 investigated runup overwash on low, flat barrier islands, experiment 2 investigated runup overwash confined through a gap in a dune and then fanning on the back barrier, and experiment 3 investigated barrier breaching. The objective of these experiments was to generate data sets to develop predictive numerical algorithms for coastal barrier overwash and breaching and to further the understanding of overwash and breaching processes.

A number of laboratory studies have been presented in the open literature (Williams 1978, Hancock 1994, Kobayashi *et al.* 1996, Parchure *et al.* 1991, Pirrello 1992, Srinivas *et al.* 1992, Baldock *et al.* 2004, Edge *et al.* 2007, and Tuan 2007), but these have focused on measuring overtopping volumes of water, overwashed volumes of sand, and beach profile changes seaward of the crest. The study by Pirrello (1992) considered wave attenuation and currents over an inundated barrier island. Such data is useful for quantifying overwash hydrodynamics during inundation overwash, although this is, as yet, to be done. To date, there have been no laboratory measurements of back barrier hydrodynamics during runup overwash and field measurements made on the back barrier during overwash occurrence (Matias 2006 and Holland *et al.* 1991) are very limited.

2.3.1 Laboratory Setup

The two-dimensional wave flume used for the experiments was 3.05 m wide, 0.9 m deep, 64 m long and was constructed of concrete. The flume had a 1:47 bottom slope extending upwards for a distance of 20.32 m at the upstream end of the flume, but otherwise the concrete bottom was horizontal (see Figure 2-1). Six consecutive glass windows provided the opportunity to view a 14.6 m length of sand barrier through the side of the flume using video cameras. The windows were positioned 9.7 m from the downstream end of the flume.

The flume was equipped with a piston type wave generator capable of generating wave heights up to 0.5 m and wave periods from 0.75 to 10 sec. A removable weir was built on the landward side of the model barrier island and downstream of this weir, a conduit was built to drain water from the operating flume into a neighbouring flume. Pumps capable of circulating approximately 22 m^3 of water per minute were installed to re-circulate water back into the upstream end of the flume.

For each experiment, a sandy barrier island was constructed in the downstream end of the wave flume. The barriers were constructed of well-sorted quartz sand with a median grain size of 0.15 mm. Three experiments were conducted on three different barrier profiles with a total of seven runs on the three profiles. Table 2-1 summarises the experiments and runs. From here on only the first two experiments are described.

Table 2-1 Experiment Runs

Profile	Run Name	Description of runs
Low flat barrier	OWB1	Runup overwash – low water level
	OWB2	Runup overwash – low water level, irregular waves
	OWB3	Runup overwash – high water level
Barrier with Dune	OWD1	Runup overwash through half-gap in side of dune (run terminated)
	OWD2	Runup overwash through gap in centre of dune
Breach Barrier with pilot channel	B1	Breaching without waves
	B2	Breaching with waves

The first barrier profile was designed to replicate a low, flat barrier island with no dune feature. The seaward slope was 1:17 and the landward slope was 1:100. Similar landward slopes are seen at Assateague Island, MD, and Metompkin Island, VA (Larson *et al.* 2004, Byrnes and Gingerich 1987). The landward slope steepened at a distance of approximately 3 m from the end of the flume, to a slope of 1:4. This was primarily done to fit the profile within the flume's length, and secondarily to recreate the bay side of an island. Wang and Horwitz (2006) describe a narrow and steep bay side shoreface for the Florida Panhandle barrier islands. Three runs were conducted on this profile. Runs OWB1 and OWB2 were conducted at a low water level with wave run up over the barrier such that runup overwash occurred, causing crest accumulation. Regular (monochromatic) waves were used for OWB1 and OWB3, and irregular waves were used for OWB2. The higher water level run, OWB3, was designed to model more severe runup overwash. Figure 2-1 shows the geometry of the flume and the barrier island profile.

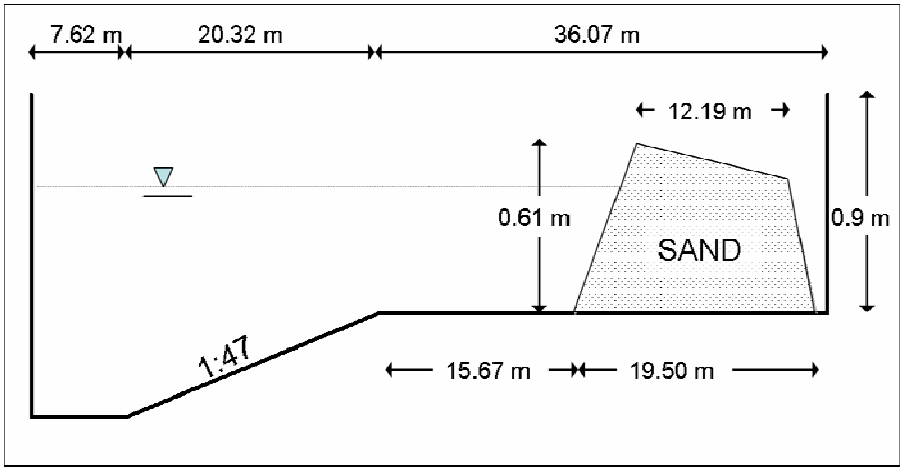

***Figure 2-1**. Sketch showing elevation view of wave flume and the sand barrier constructed within the flume (note that scale is vertically distorted).*

The dune overwash barrier profile was designed to replicate a barrier island with a prominent dune. The beach slope and back barrier slopes were retained from the previous experiment, but a dune with front and rear slopes of 1:3 and a crest width of 1.52 m, was built on top of the barrier (Figure 2-2). The dune was notched to model the channelling of overwash through a washover throat and lateral spreading of the confined overwash when it reaches the back barrier. For OWD2, the centrally located notch was 0.46 m wide and 0.38 m deep with vertical sidewalls. Another run, OWD1, had the notch located at the side of the flume but was abandoned due to excessive three-dimensional effects. The profile was modelled with a water level such that large magnitude runup overwash occurred through the dune notch. Again, monochromatic waves were used.

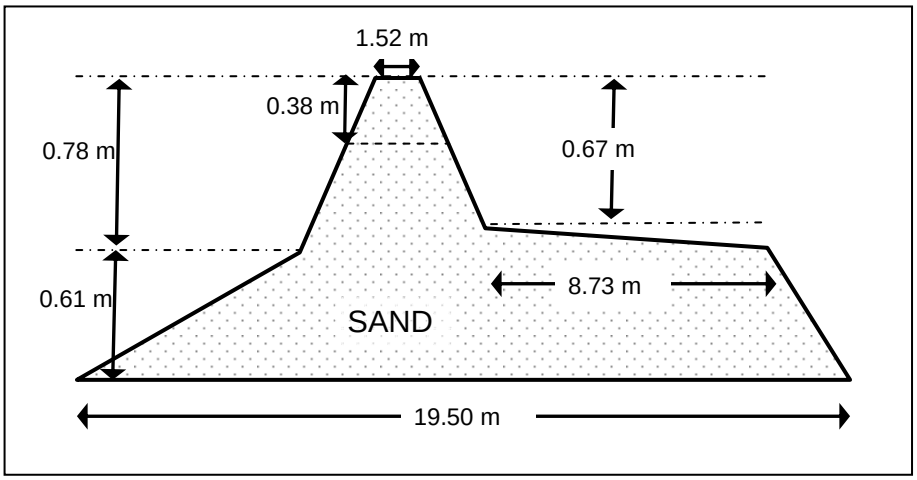

***Figure 2-2**. Sketch showing elevation view of dune barrier profile (note that scale is vertically distorted).*

2.3.2 Forcing Conditions

Table 2-2 lists the forcing conditions for the 5 different runs, including water level, wave characteristics, and run duration. To create waves with sufficient runup for overwash, long wave periods were used; hence the waves were generated in shallow water. As a result of this, some harmonics evolved as the waves broke, causing multiple peaks to be observed in

the water level signal in the swash zone. Visually, a second bore was observed to catch up with the first, after which the wave acted as a single peak event again. This caused some difficulties for analysis of the swash front velocities and depths; however, this study focused on overwash hydrodynamics, *i.e.*, at the beach crest and on the back barrier where generally, the time variation in the water level had only single peaks.

Table 2-2 Conditions for overwash experiment runs

Run	Water Level (m)	Wave Height (m)	Wave Period (sec)	Run Duration (min)	Wave Type
OWB1	0.46	0.25	7	30	Regular
OWB2	0.46	0.23 (RMS)	5	20	Irregular
OWB3	0.53	0.25	7	30	Regular
OWD1	0.76	0.23	7	abandoned	Regular
OWD2	0.61	0.23	7	30	Regular

All the runs except one were forced with monochromatic waves. The approach to the numerical modelling for which the experiments were carried out is process based and therefore, for the overwash experiments, flow characteristics on the crest and back barrier were measured for each wave. Monochromatic waves were selected to make this simpler, except for the run OWB2, which was conducted with irregular waves to quantify the differences. Most other laboratory experiments of overwash have been carried out with random waves (*e.g.* Bradbury and Powell 1992, Srinivas *et al.* 1992, Hancock 1994). Srinivas *et al.* (1992) compared the effects of monochromatic versus irregular waves for the modelling of overwash and concluded that the processes on the back barrier were similar for monochromatic and irregular waves. The main differences were in the nearshore where irregular waves were shown to diffuse the formation of a bar. For the case of accumulation overwash, accumulation of sediment on the crest is spatially more spread out, making the effect of deposition on the crest less noticeable. It should be noted that under field conditions, variations in water level due to both tidal variation and storm surge, as well as variations in wave conditions over the duration of a storm, all contribute to a variation of the overwash regimes described in Donnelly *et al.* (2006), and the morphologic change resulting from one storm can, thus, only be approximated by a single water level, wave height, or wave period representation. This mechanism was emphasised by Carter and Orford (1981).

2.3.3 Data Acquisition

Water level and bed level variation was recorded using video imagery. Digital video recordings of bed and water level variations were taken with Sony DC-42 video cameras recording in the NTSC system (USA television standard) through the 14.6 m of window along the downstream end of the flume. Each camera observed a section of the barrier profile approximately 2.8 m long through two windows. Images were sampled at a rate of 29.97 Hz and each image has a resolution of 720 x 480 pixels where 1 pixel represents approximately 4 mm (this varied slightly between runs and cameras). The extracted bed and water levels were used to calculate water depth, wave front velocity, runup slope and bed level variation during the runs.

Image rectification and scaling was made possible by recording measured grids of squares in the plane of the windows prior to starting the runs. Water and bed levels were then extracted using the Canny edge detection algorithm (Canny 1986). The method used for image analysis was based on that described by Erikson and Hanson (2005). The method and

potential accuracy is described in further detail in **Paper V**. Only overwashing waves which exceeded 2 pixels in height were analysed such that the potential error in determining the water depth did not exceed the water depth itself. It is believed that the ability to analyse such data at high spatial and temporal resolutions outweighs the potential errors.

Additionally, pre- and post-run surveys of the barrier were taken for all runs. Surveys were taken with a total station with an accuracy of +/- 2 mm mean squared error. Three cross-shore lines were surveyed, the profile centreline, and a distance of 3 cm from each of the flume side walls, corresponding with the locations of the instrumentation described below. These survey lines were defined as “north”, “centre”, and “south”, where north is the right hand side of the flume looking downstream.

In addition to the video imagery analysis, capacitance wave gauges (CWGs) sampling at 20 Hz measured water level variation on the ocean side of the constructed barrier, and on the foreshore, dune crest and back barrier. An array of three CWGs measured the water level upstream in the flume to calculate wave reflection and extract the incident wave time-series using the Mansard and Funke (1980) three-probe wave reflection analysis. Wave gauges on the profile were buried to ensure that data was still collected as the profile eroded. These gauges were therefore periodically dry between each wave. Data from the buried wave gauges gives some indication of water and bed level variation, but comparison of this data with water levels extracted from video image analysis indicated that the gauges usually recorded a draw-down of the water level in the sand barrier when the barrier surface was dry, hence the data was not used. Also, some buried gauges were washed out by scour during the runs or recorded too high water levels where large amounts of bubbles were present.

An attempt was also made to measure the current velocity at the foreshore, the dune crest, and the back barrier beach using Sontek Acoustic Doppler Velocimeters (ADVs) sampling at 10Hz. The ADVs in the swash zone and landward of the swash zone were subject to cyclical wetting and drying, and significant turbulence in shallow depths. Because of this, the signal to noise ratio and correlation coefficients of the recorded signals was such that the recorded data could not be used.

2.3.4 Observations: Low flat Barrier Experiment

Experiment run OWB1, modelling runup overwash on a low, flat barrier island resulted in removal of sand from the foreshore, deposition on and immediately landward of the crest (crest accumulation), and very little change on the back barrier slope. On the steep rear slope supercritical flow occurred. The first few waves to overwash the barrier infiltrated into the relatively dry backbarrier very quickly; hence the velocity of the landward flow decreased rapidly and the penetration of the landward flow was small (Figure 2-3). Both the landward flow velocity and the landward flow penetration, however, increased with each subsequent wave until the barrier was saturated. The barrier was considered saturated when a small film of water was always visible on the back barrier. Despite the fact that flow was eventually observed to penetrate the entire modelled barrier length, morphologic change was limited to the barrier crest. Observations of the runs through the flume side window revealed suspended sediment and bedload in the uprush bores, but relatively clear flow both landward of the barrier crest and in the backwash flow, indicating that relatively low energy overwash results in crest accumulation.

Processes observed during OWB2 were very similar to those observed during OWB1, but due to the irregular forcing conditions, the occurrence and magnitude of waves large enough to overwash the barrier was also irregular. Because of this, the back barrier took

significantly longer to become saturated which may be a real issue in field conditions. The irregular runup extent resulted in a higher spatial variation in the location of the sand deposited on the barrier crest than in OWB1. The surveys show negligible bar development, only a small accumulation of sediment on the barrier crest, and a minor steepening of the rear barrier slope. The beach change was fairly two-dimensional. Therefore, the most obvious differences between the monochromatic and irregular wave runs were that the nearshore bar and accumulation on the barrier crest were more dispersed.

***Figure 2-3**. One of the first waves during OWB1.*

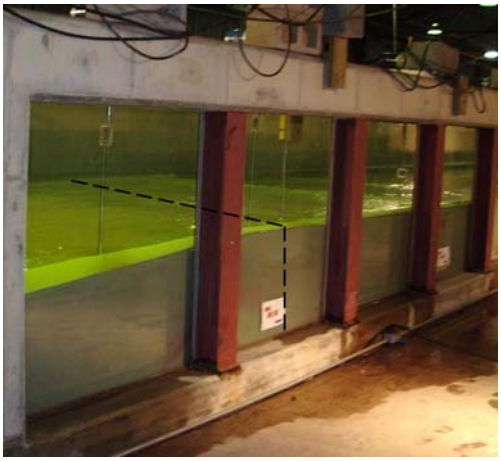

***Figure 2-4**. Cross-shore profile during run OWB3. The direction of wave propagation is to the right.*

Overwashing bores in run OWB3 were significantly larger and more energetic than those observed in OWB1 and OWB2. The crest was overwashed initially by a thin wedge of water, followed by a broken bore front. Figure 2-4 shows overwash during OWB3. Suspended sediment and bed load was observed in the uprush and overwashing flow, in particular directly behind the broken bore front. Flow on the back barrier was constant and small sand ripples formed and migrated upstream. As for the previous experiment runs, flow accelerated significantly on the steeper rear slope causing antidunes to form and migrate, eventually causing the entire rear back slope to migrate seawards and become less steep. The surveys show negligible bar development, landward migration of the dune crest, and steepening of the rear barrier slope, caused by supercritical flow over the rear end of the profile.

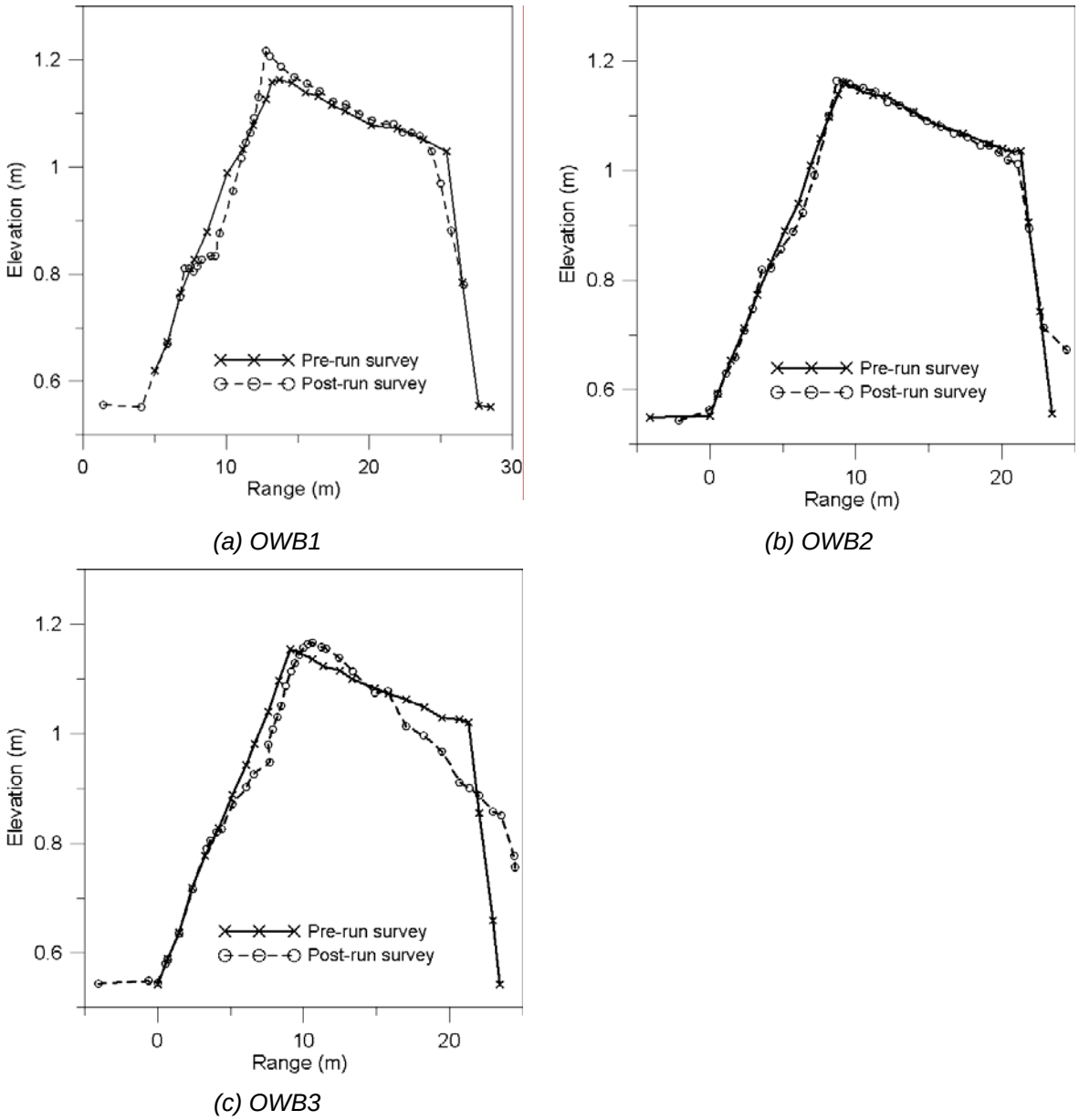

***Figure 2-5**. Pre- and post- run surveys along flume centreline for runs (a) OWB1, (b) OWB2, and (c) OWB3. The direction of overwash flow is from left to right.*

Figure 2-5 shows the cross-shore surveys along the flume centreline before and after the three low flat barrier experiment runs. In summary, for all runs an accumulation of sediment on the barrier crest, and steepening of the back barrier slope was seen. The beach change was reasonably two-dimensional, except on the rear slope where channels formed. The steeper rear slope became less steep and migrated seawards. This effect was most pronounced for run OWB3; however, analysis of these back barrier hydrodynamics for these runs was restricted to the unaffected upper part of the back barrier slope.

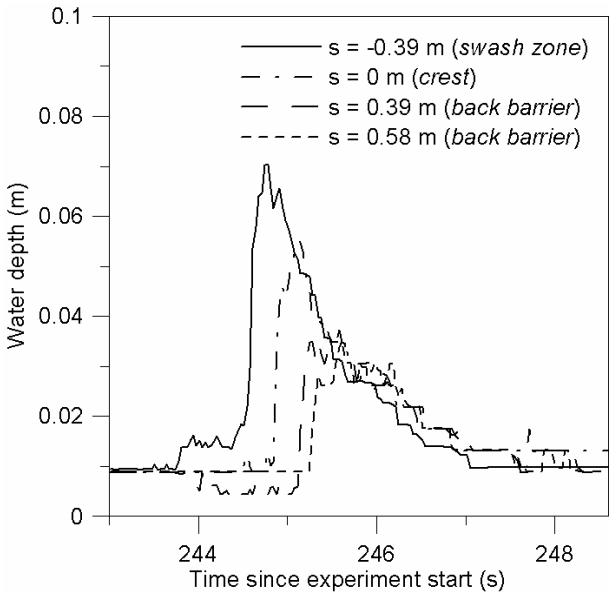

***Figure 2-6**. Time variation of water depth at various positions on the barrier, run OWB3.*

The hydrodynamics observed during this experiment are discussed in **Paper V**. Water level data from the digital video image analysis was used to study the time and spatial variation of water depth and the spatial variation of the wave front velocity. Only results from OWB1 and OWB3 are presented here. Camera failure at the beach crest limited the data from OWB2, and the central location of the notch for OWD2 meant that water and bed surfaces were not visible to the cameras. Figure 2-6 shows the time variation of the water depth during a single overwashing wave at various positions on the barrier. The shape of the event is similar from the swash zone to the back barrier, despite the division of flow into backwash and overwashing flow around the beach crest. The overwashing wave height, H_{ow}, (maximum depth at a point during a single wave event) reduces with distance along the barrier, and the peak becomes broader. The reduction in overwashing wave height, down the back barrier, normalised by the wave height at the crest, H_c, is shown in Figure 2-7 for experimental runs OWB1, OWB3 and field data recorded by Holland *et al.* (1991). Note that the reduction in wave height is linear and similar for all data sets in the swash zone, but varies on the back barrier. Figure 2-8 shows the actual (non-normalised) overwashing wave height variation on the back barrier. It appears that a similar minimum wave height is approached by all three data sets, but at a different rate. It is possible that the minimum wave height represents the normal flow depth for a particular slope, because all three data sets represent similar back barrier slopes.

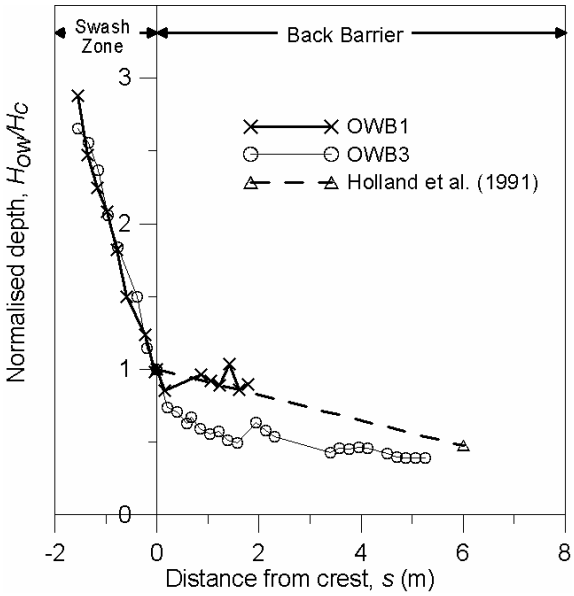

***Figure 2-7**. Average normalised wave height versus distance from crest*

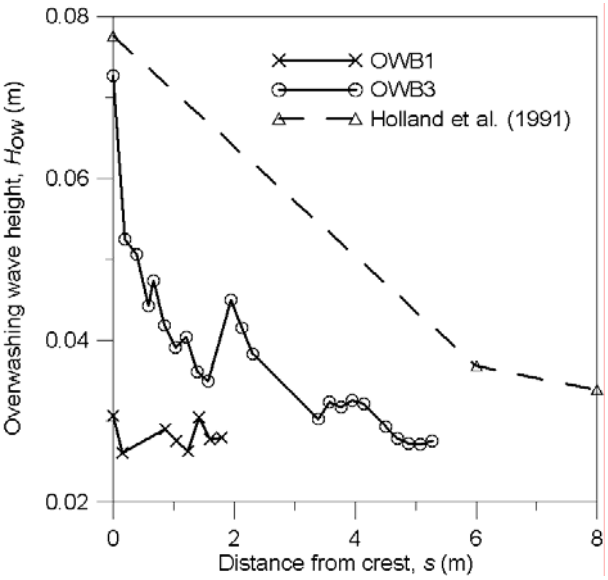

***Figure 2-8**. Average overwashing wave height versus distance from crest*

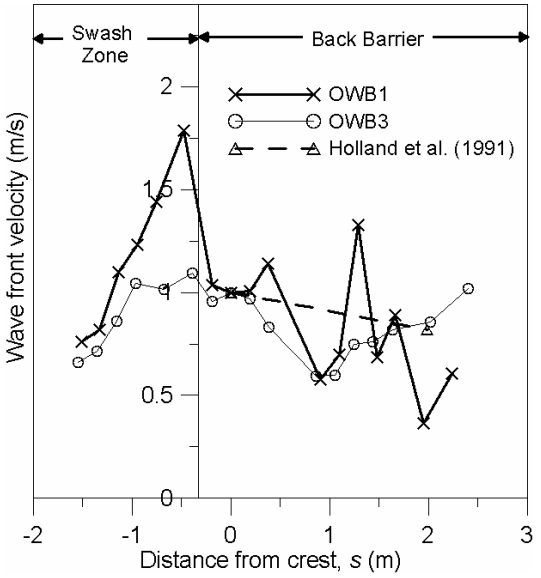

***Figure 2-9**. Average normalised wave front velocity versus distance from crest*

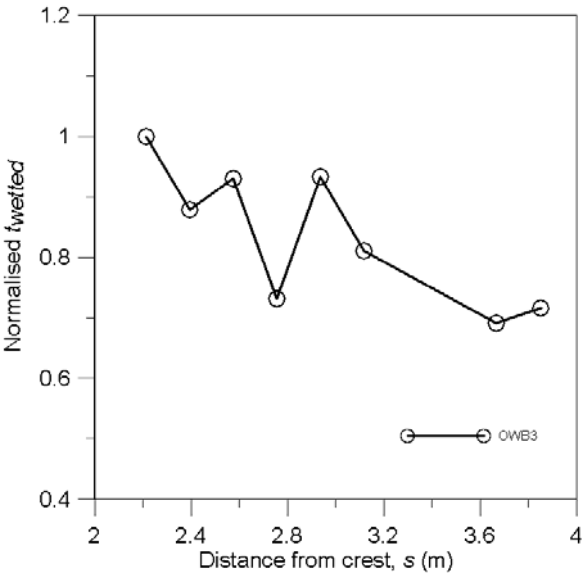

***Figure 2-10**. Spatial variation in normal t_{wetted} for the back barrier*

Figure 2-9 shows the spatial variation in overwash wave front velocities for experiment runs OWB1, OWB3 and the Holland *et al.* (1991) field data. The swash front velocities were calculated using the time of bore arrival at two different gauges (**see Paper V**). Because the ADVs did not function in the shallow, unsteady overwashing flows, Eulerian flow velocity data is not available. Of interest is the swash front acceleration seen in the swash zone for both experiment runs. In the swash zone, this is thought to indicate strong initial pressure gradients accelerating the newly formed swash front (Hughes and Baldock, 2004). It is suggested that because theoretical runup levels and wave periods must be large for overwash to occur, a larger than normal region of swash zone acceleration exists during

overwash. This is of significance to sediment transport and profile change in the swash zone during overwash. On the back barrier, the flow field for the OWB3 data is affected by the 'catch-up' of the 2nd harmonic wave at about s = 1 m, where s is the distance from the beach crest on the back barrier. Seaward of this point, the decelerating trend seen is that of the first wave front and landward of this, the accelerating trend is that of the combined waves. The OWB1 data possibly shows a trend of flow deceleration, but this was not clear from the data. The overwashing wave height in this run was small in comparison to the thickness of the film of water remaining on the barrier surface between wave events, meaning that surface bubbles were seen to affect the overwash flow, and hence the overwash flow velocities. This data was therefore not further analysed.

Two new parameters were defined to analyse the time variation of the flow depth along the back barrier. The wetted duration, t_{wetted}, represents the period over which a single overwashing wave has a depth > 0 m, and the second, t_{max}, represents the period over which the water depth is increasing during a single overwashing wave, *i.e.*, the time between the arrival of the wave front and the time of peak water depth for that wave. Assuming that the wave shape in the time domain, seen in Figure 2-6, can be approximated as a triangle, these two parameters and the overwashing wave height define that shape. This approach was inspired by that taken by Tuan (2007) for determining the asymmetry in overtopping flow rates. It is of interest to observe how this shape attenuates down the back barrier. Figure 2-9 indicates a slight decrease in t_{wetted} for the OWB3 data as the overwash wave progresses down the back barrier. There was no significant trend in the spatial variation of t_{max} down the back barrier; however, the error in determining t_{max} from the video data may have been of the same order of magnitude as the changes in t_{max}. Visually, it does appear that the wave front steepens down the back barrier, as may be expected for a shallow water wave. A steeper wave front means more rapid velocity accelerations as the overwash wave arrives at a point, hence a higher potential for sediment entrainment and transport. These simple results highlight the need for further measurements of overwashing flow on the back barrier. In particular, measurements of the Eulerian variation in velocity during each wave would be useful for calculating sediment transport and flow rates on the back barrier.

2.3.5 Observations: Fanning Overwash Experiment

The purpose of this experiment was to observe processes during overwash through a gap in a line of dunes (hereafter referred to as a washover throat), and the lateral spreading of that overwash behind a low flat barrier. A further outcome of these experiment runs was the opportunity to observe the initiation of breaching. An initial run of this experiment (OWD1) with a notch located along the flume wall was abandoned. The idea was to model one half of an overwash fan so that water depths and bed level change could be observed through the flume window; however, three-dimensional effects made the run non-representative of field conditions. For the second run, OWD2, the washover throat was relocated to the flume centre.

Figures 2-11 to 2-16 show various aspects of the flow at different times throughout the experiment run. In the initial stages of the run the dune face on either side of the flume was scarped by waves while overwash penetrated the washover throat, notching the throat sides and spreading laterally on the back barrier (Figures 2-12 and 2-14). The lateral spreading angle increased with each subsequent bore until the back barrier was saturated, and the laterally spreading overwash formed a nearly circular fan on the back barrier (Figure 2-13), depositing sand as it spread. Approximately four minutes into the run, slumping of sand from the sidewalls of the washover throat blocked the throat from further overwash. Slumping occurred due to notching of the sidewalls in the throat (Figure 2-15). While the

throat was blocked, the wave runup continued to widen the throat entrance and eventually eroded the slumped sand allowing overwash to once again penetrate the throat.

***Figure 2-11**. OWD2 profile prior to experiment start. Direction of flow is from bottom to top of picture.*

***Figure 2-12**. First overwashing wave on the dunes and through the washover throat*

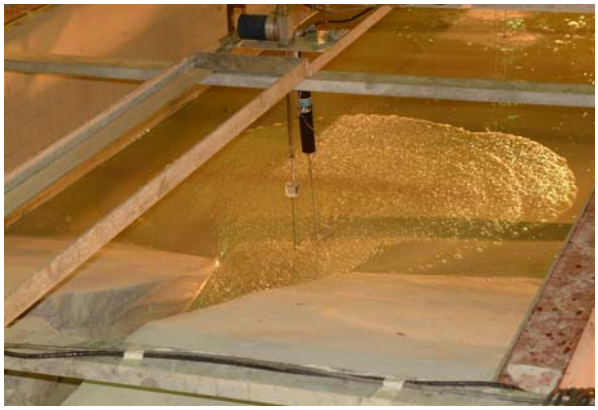

***Figure 2-13**. Lateral spreading of overwash on the back barrier*

***Figure 2-14**. Notching and sediment slump in washover throat and sediment slump on dune face.*

***Figure 2-15.** Slumping of sediment in washover throat and scarping of the beach face*

***Figure 2-16**. Supercritical flow into washover throat, hydraulic jump at bottom, widening of throat (Photos taken by Ken Connell)*

Approximately 14 minutes into the run, the flow down the landward side of the dune (immediately downstream of the throat) became supercritical. The supercritical flow

scoured a large hole at the landward end of the washover throat. The slope on the seaward side of the scour hole was steep (approximately 45 degrees) and migrated seaward, maintaining this slope and deepening the notch. At the same time, erosion continued on the seaward side of the dune until eventually the washover throat formed a channel below the water level (Figure 2-16). Inundation overwash then began through the throat which then widened rapidly. These observations have significance for the destruction of dunes when overwash is confined through a throat and possibly for the initiation of breaching.

Figures 2-17 and 2-18 show the pre- and post-run surveys along the edge and centreline of the flume, respectively. Note that along the flume sides, the dune retained its height but became narrower due to scarping. The sediment gain on the back barrier was deposited by lateral spreading, and not over the crest. Along the centreline of the flume, the washover throat was significantly lowered until no prominent dune form was recognisable. Inland penetration of sediment on the back barrier was further along the centreline than along the edges of the flume, and the deposited sediment was deeper.

Hydrodynamic data collected on the beach crest and back barrier during this run was limited. Due to the location of the notch in the middle of the barrier it was not possible to record water depths and bed level variations in the notch using video imagery analysis. Buried CWGs recorded water level and bed level variation in the centre of the washover throat, and at various positions on the back barrier. Buried wave gauges may show both the variations in water level, and in cases where the gauge is subjected to drying, the variation in bed level. The time-series recorded by the CWG indicates that the water level always dropped down to a minimum value, physically determined by the interface between sand and water. This minimum value varied slowly as sand was either removed from or added to the gauge location. The time-variation in the minimum value should therefore represent the time-variation of the bed level. After determining this level, it may be subtracted from the time-series to give the water-depth time series. This was also done for the first experiment runs, OWB1, OWB2 and OWB3, and compared with the water levels determined using video image analysis. This technique overestimated water depths due to draw-down of the water level between overwash waves and the gauges overestimated water levels due to the recording of bubbles and foam as the top of the water level. This effect, however, decreased with distance down the back barrier, or in other words with decreasing wave height. It is therefore acknowledged that the water depths and bed levels presented here for OWD2 are somewhat limited in their accuracy, but are included to show the qualitative spatial and temporal variation of bed level and water depth.

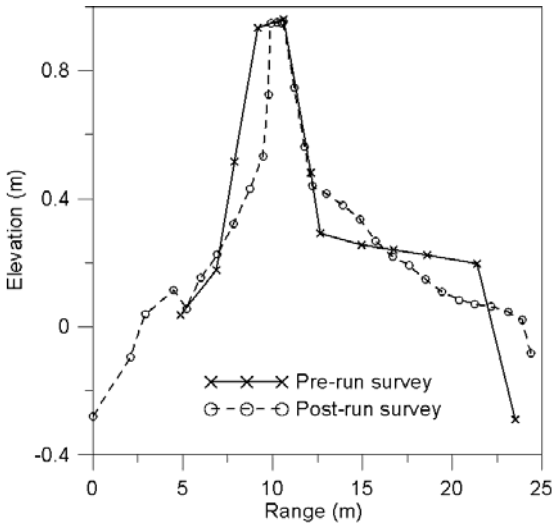

Figure 2-17. *Pre- and post-run surveys, OWD2, north side of flume. The direction of overwash flow is from left to right.*

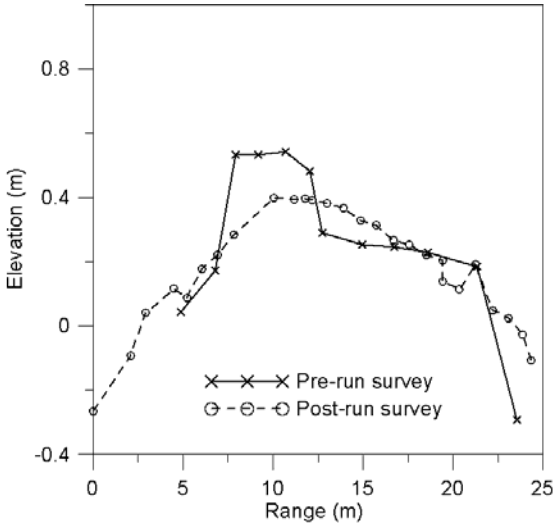

Figure 2-18. *Pre- and post-run surveys, OWD2, centre of flume. The direction of overwash flow is from left to right.*

Figure 2-19 shows the approximate variations in bed level at (a) the centre of the washover throat, *i.e.* the beach crest, (b) immediately downstream of the washover throat, and (c) further downstream on the back barrier.

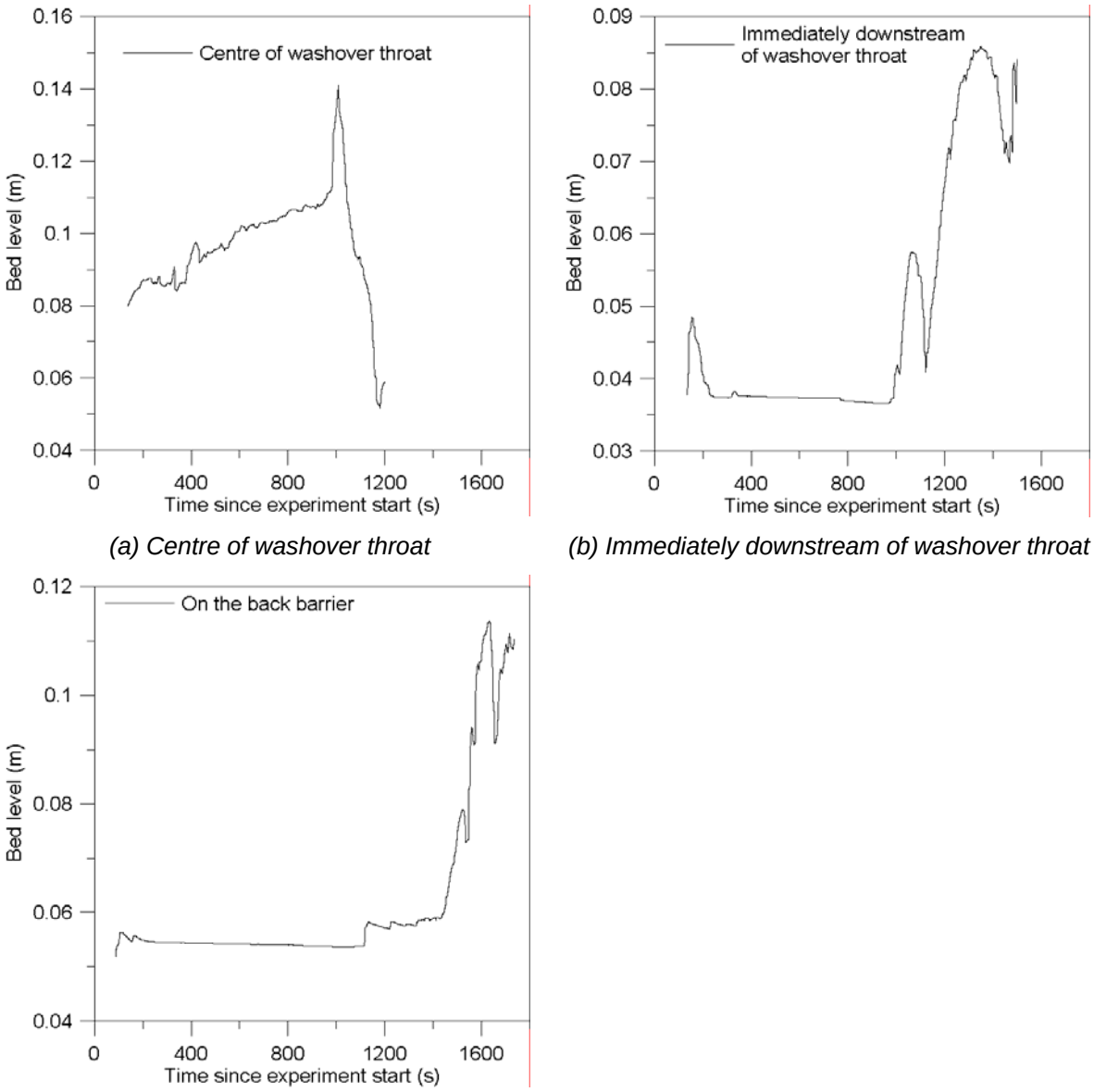

(a) Centre of washover throat

(b) Immediately downstream of washover throat

(c) On the back barrier

***Figure 2-19**. Bed level variations during experiment run OWD2*

Once the barrier is saturated, the time-series give an indication in the bed level trends. The bed level in the washover throat (Figure 2-19a) increased gradually for most of the run. This was at least partly due to slumping and reworking of sediment in the throat. It cannot be deduced how much, if any, of this sediment deposition originated from the beach face. After around 1200 sec, the gauge was washed out, so the bed level cannot be calculated. Immediately downstream of the washover throat and further down the back barrier (Figures 2-19b and 2-19c), there is a small amount of deposition, caused by the deceleration of the

flow on the back barrier. The washover throat, however, was blocked for a large period of time, hence the period of no change. The changes in bed level became rapid at the end of the run as the throat became inundated.

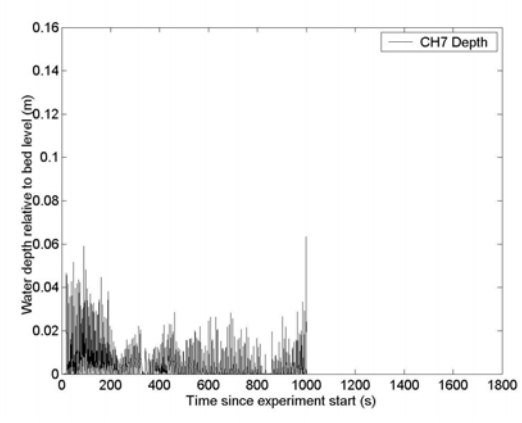

(a) Centre of washover throat

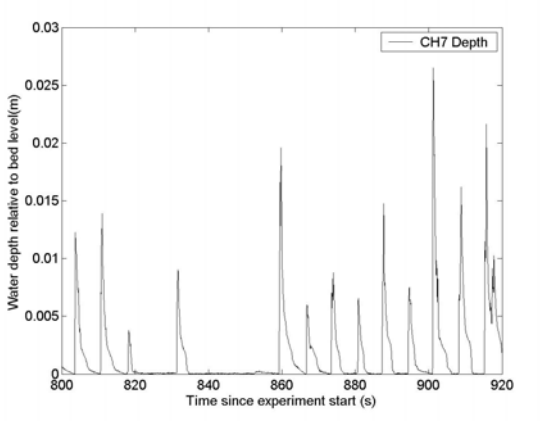

(b) Centre of washover throat – detailed view

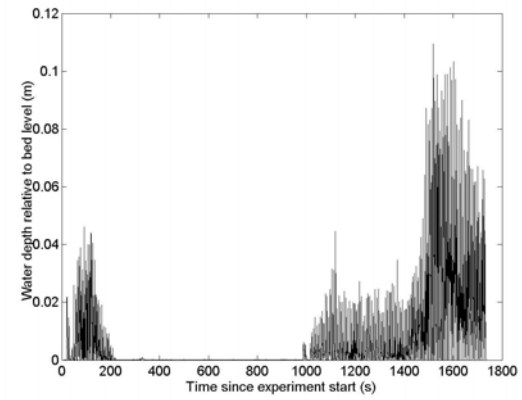

(c) Immediately downstream of washover throat

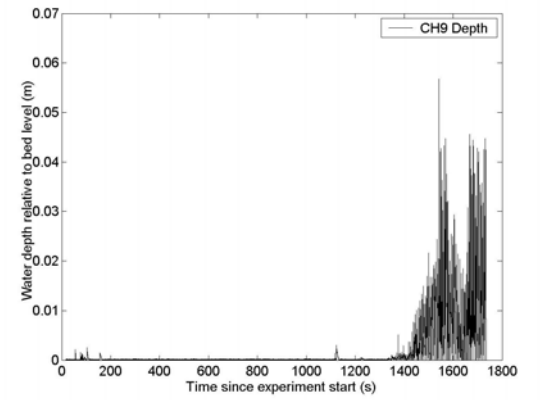

(d) On the back barrier

***Figure 2-20**. Depth time-series during experiment run OWD2 (note vertical scales vary)*

Figure 2-20 shows the water depth variations in and near the washover throat and on the back barrier during the OWD2 run. Only the first 1000 s of water level variation were recorded in the washover throat, due to washout of the gauge. Even though the forcing waves were monochromatic, the water depth signal in the throat is somewhat irregular (*e.g.* detailed view in Figure 2-20b), due to blocking of the throat by slumped sand. On the back barrier (Figures 2-20c and 2-20d), there is a period at the start of the run in which overwashing waves were recorded. These were substantially smaller in depth by the time they reached the back barrier gauge, 3.9 m downstream. After 1000 s, the washover throat became inundated and larger waves reached the back barrier, although a decrease in depth between the two gauges was still observed. The results indicate a decrease in water depth with distance down the back barrier, and a large increase in water depths everywhere as the overwash regime changed from runup to inundation overwash. Following the increased water depths more rapid changes in bed level were recorded.

In summary, overwash confined through a gap in a dune was seen to be an unsteady process due to the irregular slumping of sediment into the washover throat, blocking overwash penetration. Wave by wave, process models of overwash therefore need to consider sediment slumping in the washover throat. The presence of a rear dune slope causing supercritical flow was also seen to be an important overwash process, migrating seawards and regulating flow velocities on the back barrier. The reduction of slope on the back

barrier, lateral spreading and skin friction caused sufficient flow deceleration for the deposition of sediment on the experimental back barrier.

3 Overwash Processes

Overwash processes refers to the physical processes that affect the flow hydrodynamics and sediment transport caused by overwash. Many descriptions of overwash occurrences exist in the open literature and several different processes have been described as overwash. What all these processes have in common is the transport of water and sediment over the beach crest; hence the decision here to refer to all such processes as overwash. Overwash may further be categorised based on the overwash regime (forcing processes, including incipient morphology) and the back barrier processes. Much of the literature pertaining to overwash is restricted to description of singular overwash events or the long-term role of overwash in barrier dynamics, rather than general descriptions of overwash processes; however, some attempts have been made to relate observed post-storm morphologies to forcing processes and back barrier processes. In this thesis previous work on overwash processes, new conclusions regarding overwash processes derived from the published literature (**Paper I**), morphologic categorisation of washovers (Donnelly et al. 2006, **Paper II**), and new conclusions regarding overwash processes on the back barrier derived from pre- and post-storm topographic observations in combination with the associated forcing (**Paper VI**), are described.

Previous work done on identifying the processes that affect washover deposition include: relating the stratigraphy of sediments deposited by overwash to the deposition environment, *i.e.* subaqueous or subaerial (Schwartz 1978); the effects of wind forcing on washover deposition (Morton 1979); defining hydrodynamic overwash regimes (Sallenger 2000); correlating distances of landward overwash penetration with different factors such as washover morphology type and forcing (Morton and Sallenger 2003); and comparisons of washover stratigraphy deposited in regions without vegetation and with different types of vegetation (Wang and Horwitz 2006).

Donnelly *et al.* (2006) categorised the cross-shore beach profile changes caused by overwash into seven different cross-shore morphology change types. More than 110 sets of pre- and post-storm cross-shore beach profiles showing overwash occurrence were assembled and some consistencies in the morphologic response of the profiles were observed; hence, the responses were categorised.

Plotted at the same scale, the profile sets were grouped according to similarities in morphologic change landward of the beach crest and as to whether or not a dune existed on the pre-storm beach profile. A dune was identified as a prominent feature on the profile, with the slope on the rear of the dune exceeding 1:20 and a height exceeding 0.5 m above the back barrier. These simple geometrical definitions made it possible to objectively determine when a prominent feature existed.

The seven different morphology change types observed were crest accumulation, landward translation of dunes and berms, dune lowering, dune destruction, barrier accretion, short-term barrier rollover, and barrier disintegration. Examples of each change type are shown and discussed in Donnelly *et al.* (2006). Figure 3-1 shows schematically the different change types identified, which are discussed below.

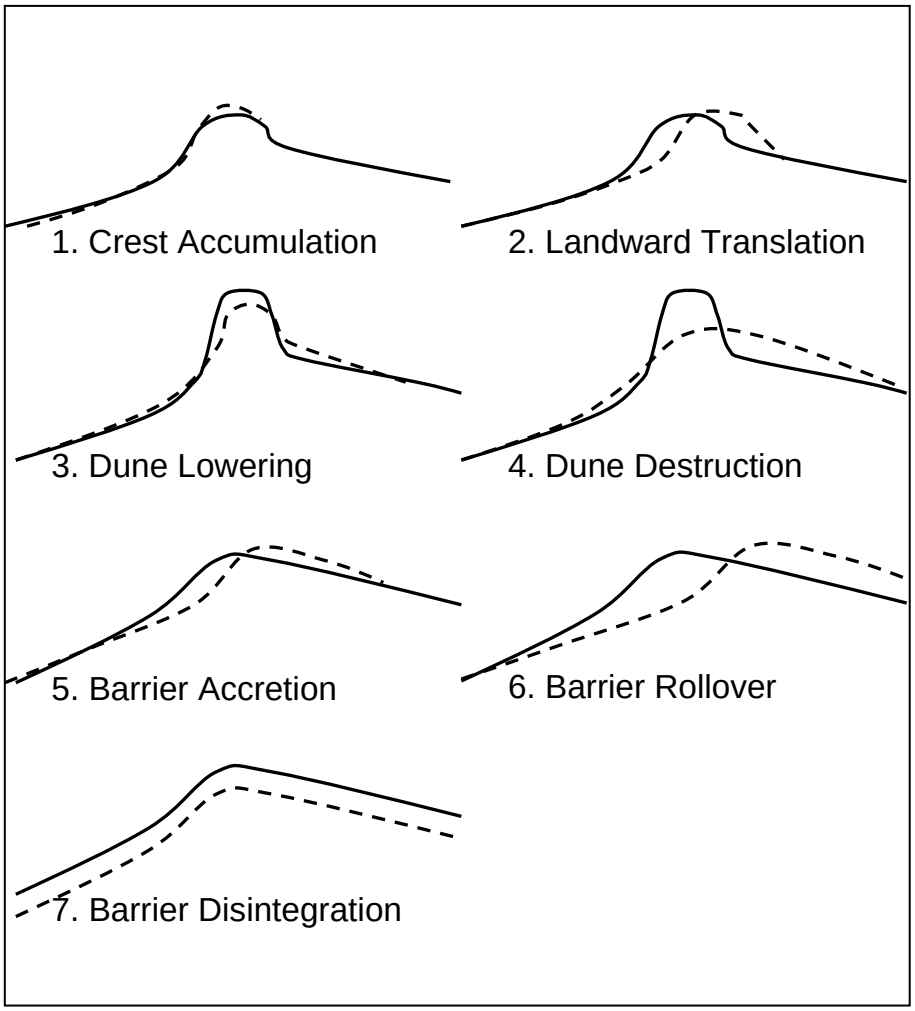

***Figure 3-1**. Schematic showing cross-shore profile responses to overwash. The dotted line indicates the profile after an event. The ocean is to the left.*

1. Crest Accumulation: This is the accumulation of sediment on the beach crest. The phenomenon was first described in terms of overwash by Fisher *et al.* (1974) and by Leatherman (1976), and was observed on shingle beaches by Carter and Orford (1981). As the runup decelerates up to the beach crest, sediment is deposited. The overtopping flow may continue over the crest.

2. Landward Translation of Dunes/Berms: A landward translation of an intact dune is observed both for prominent foredunes and for less prominent beach berms. The dunes usually maintained their height above sea level, but cases where the dunes slightly increased or decreased in height were also observed.

3. Dune Lowering: A reduction in dune height and volume is observed. Sediment is removed from the seaward side and crest of the dune and a portion is deposited behind the crest in a wedge decreasing landward. Thus, the dune crest height is reduced, while the back barrier height increases. Dune lowering is the predecessor of dune destruction.

4. Dune Destruction: A prominent dune is no longer observed on the post-storm profile. The entire foredune has been destroyed. A portion of the dune's sediment is usually deposited behind the original crest position in a landward-decreasing wedge. The proportion of sediment deposited on the barrier depends on the amount of dune erosion that occurred prior to overwash. Both situations where most of the dune sediment and only a portion of the dune sediment are deposited as washover have been observed.

5. Barrier Accretion: On a beach without a prominent dune, washover is transported from the beach face and beach crest and deposited on the subaerial portion of the island. The barrier therefore becomes narrower and higher, and the rear slope becomes steeper. The landward extent of washover does not reach the back barrier bay. It should be noted, however, that it is possible that the sediment was deposited subaqueously when the back barrier water levels were elevated during the storm.

6. Barrier Rollover (short-term): A washover deposit extending from the subaerial portion to the subaqueous bay-side of the island is observed. This indicates the landward translation of an entire barrier island or spit. It refers to the short-term rollover caused by a single overwash event (barrier rollover is often discussed at geological time-scales). During an overwash event, sediment is transported from the foreshore and deposited both on the rear barrier slope and in the back barrier bay. Where foredunes exist, these are destroyed prior to inundation, indicating some cross-over between the responses.

7. Barrier Disintegration: Erosion is observed over the entire subaerial barrier island or spit. This occurs when low-lying barriers become completely inundated. Sediment is removed from the entire barrier island surface in high-energy overwash conditions and either deposited subaqueously near the rear side of the barrier or lost offshore. If this continues for a sufficient length of time, the barrier may breach such that the post-storm profile lies below mean sea level.

Chapter 5 and **Paper II** discuss how these morphologic categories relate to the forcing processes.

3.1 Forcing Processes

Sallenger (2000) and Morton and Sallenger (2003) recognised that two hydrodynamically different processes were responsible for post-storm morphologic change on back barriers, namely excess wave runup over the beach crest, and water levels exceeding the beach crest. Sallenger (2000) named these ‘overwash regime’ and ‘inundation regime’ in his Storm Impact Scale, which provides a simple method for predicting overwash occurrence and magnitude. Since, however, many other authors have also referred to ‘inundation’ as ‘overwash’ (*e.g.* Dolan and Godfrey 1973, Weir 1977, Byrnes and Gingerich 1987, Leadon 1999), the terms *runup overwash* and *inundation overwash* were introduced in **Paper I** to describe the two different forcing regimes causing morphologic change landward of the beach crest. Figure 3-2 shows an example of washover deposited by both regimes. Figures 3-3 and 3-4 show schematic cross-sectional depictions of a barrier subject to runup and inundation overwash, respectively. Runup and inundation overwash may occur during the same storm, either simultaneously due to local spatial variations in beach crest height, or sequentially due to temporal variations in water level, a fact that should be taken into account when trying to relate observed washover morphology to a forcing regime.

***Figure 3-2**. Washover caused by runup overwash regime (foreground) and inundation overwash regime (background) on Assateague Island following 1998 northeaster storms (photo Don Stauble).*

The forcing mechanisms related to the seven different response types identified by Donnelly *et al.* (2006) are the overwash regime, the storm surge level, wave conditions, incipient beach profile, and the storm duration. The barrier responses (barrier accretion and short-term barrier rollover), require longer storm durations than the less severe morphology change types (crest accumulation, landward translation, and dune lowering and destruction) (**Paper II**).

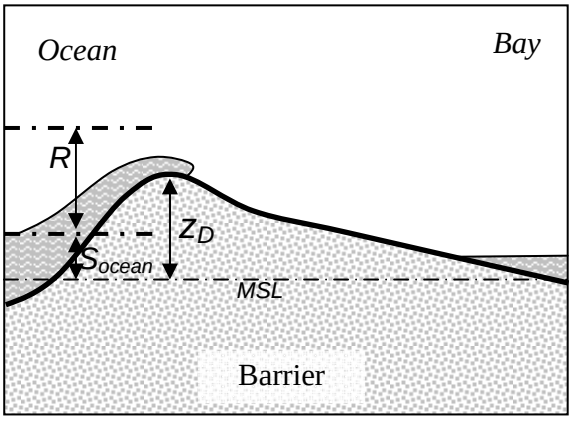

***Figure 3-3**. Schematic of a barrier undergoing runup overwash*

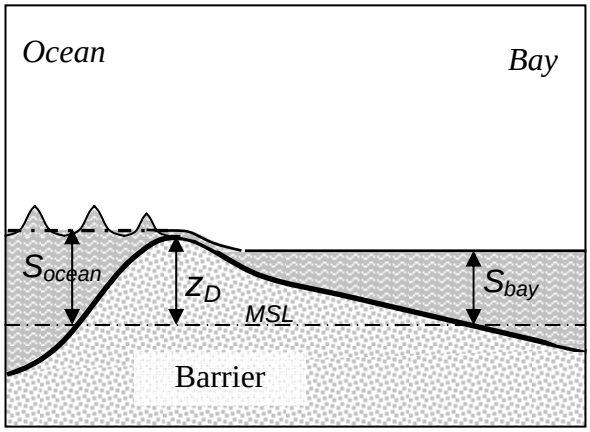

***Figure 3-4**. Schematic of a barrier undergoing inundation overwash*

3.1.1 Runup Overwash Forcing

Runup overwash occurs when the mean water level (including surge) is below the beach crest elevation, but the beach crest elevation is exceeded by wave runup. Runup overwash may be thought of as a swash bore that continues over the beach crest and down the other side. It should be noted, however, that a portion of the swash returns down the beach as backwash, as observed in the experiments. In **Paper II** it was shown that the relative elevations of the beach crest height, z_D, and the water level including storm surge, S_{ocean}, are the important forcing processes determining the magnitude and type of morphology change observed during runup overwash. For example, crest accumulation occurs for the limiting condition when the water level and runup level are sufficient for overwash occurrence, but the velocity of the uprushing wave on the beach crest is such that sediment is deposited on the beach crest during overwash. Interestingly, the variation in the runup height, R, had little effect on whether or not accumulation overwash occurred, once the threshold for overwash occurrence was exceeded (**Paper II**). At larger values of S_{ocean}, more erosive morphology changes were observed, and the runup height becomes more important in determining the type of morphology change observed. For example, the landward translation of a dune or berm occurred only for a restricted range of runup values. Dune lowering and dune destruction occurred for similar forcing conditions to crest accumulation, but generally for narrower dunes only. The relationships between various overwash morphologies and the forcing mechanisms are further described in Chapter 5 and in **Paper II**.

3.1.2 Inundation Overwash Forcing

Inundation overwash occurs when the mean water level including storm surge exceeds the beach crest elevation. This may either occur locally, *i.e.* through a washover throat, such that the overwash flow subsequently fans out onto the back barrier, as was observed towards the end of experiment run OWD2, or over a larger alongshore region such that sheetwash (spatially unconfined overwash) occurs, as was observed on the western end of Santa Rosa Island during Hurricane Ivan (**Paper VI**).

When inundation overwash occurs on barrier islands, coupling between the ocean and bay water levels can occur. Often, there is a time lag and elevation difference between the ocean and bay water levels, such that a water level gradient driving the flow from ocean to bay exists. In this case, the overwash forcing may approximately resemble steady open-channel flow. The waves also contribute to the hydrodynamic processes, although rather than run-up processes, the wave action is dominated by shallow-water processes such as wave breaking and reformation. Despite the wave action, it is suggested that the water level gradient is the dominant process for inducing morphologic change during inundation overwash. Pirrello (1992) conducted several experiments simulating inundation overwash in a flume both with and without an induced water surface gradient current. A large increase in volume of sediment transported landward was seen for the water surface gradient cases, and comparison of the velocity profiles for the two profiles indicated more vertically uniform landward currents for the water gradient cases. In particular, the current near the bed, hence the capacity for eroding sediment, was much stronger for these cases. It was therefore concluded that the water surface gradient, rather than wave induced currents, is the driving force behind large scale sediment transport. When inundation overwash occurs, the duration of the inundation is also an important factor in determining the resulting morphologic change (**Paper II**).

3.2 Back barrier Processes

The shape, position and extent of washover deposits varies greatly depending on the magnitude of the overwash event and a number of different back-barrier processes. These back barrier processes include lateral spreading, hydrodynamic changes affected by back barrier topography (slope, existence of rear dune ridges or other slope irregularities, existence of channels, etc.), the surface texture of the back barrier (*i.e.* friction caused by vegetation, urban development, grain size, etc), proximity to a back barrier bay, and saturation and ground water levels on the back barrier. These processes generally cause a decrease in the sediment carrying capacity of the flow on the back barrier, and hence, deposition of sediment. In general, as the velocity of the flow on the back barrier decreases, sediment is deposited due to the cross-shore gradient in sediment transport. In **Paper VI**, a combination of pre- and post-storm data, aerial photography and storm surge levels were used to determine the processes active on the back barrier and their relative importance.

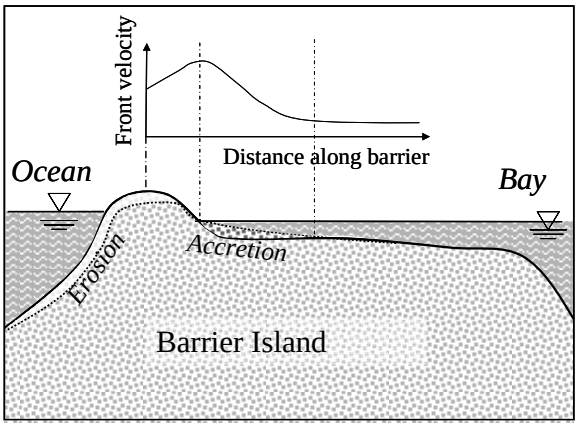

***Figure 3-5**. Schematic of subaqueous deposition starting at the bay water level interface*

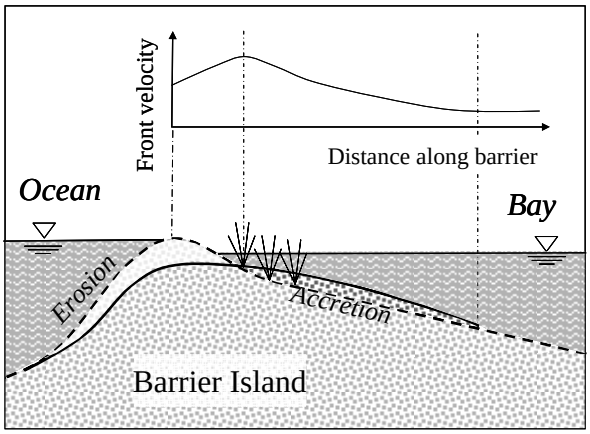

***Figure 3-6**. Schematic of subaqueous deposition landward of bay water level*

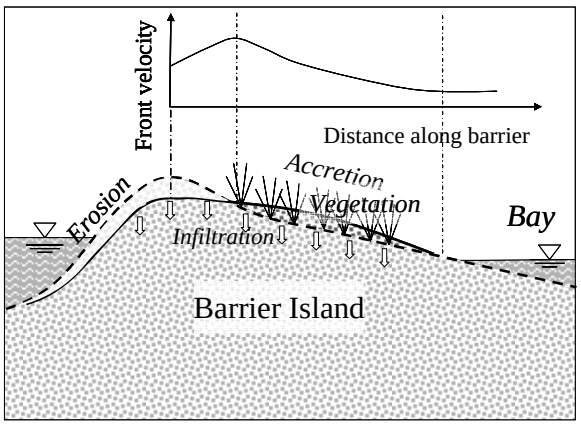

***Figure 3-7**. Schematic showing subaerial overwash deposition processes*

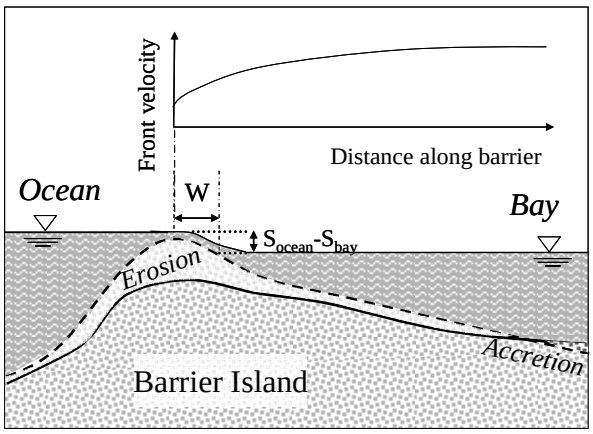

***Figure 3-8**. Schematic showing barrier disintegration due to inundation overwash*

Figures 3-5 to 3-8 schematically show how several different back barrier processes act to decelerate flow and enhance washover deposition. Subaqueous deposition of overwash starting at the bay water level interface with the back barrier is shown in Figure 3-5. It was seen that a transition from acceleration to deceleration of the overwash flow occurs where the bay water level meets the back barrier (**Paper VI**). Flow accelerates subaerially down the back barrier from the beach crest until it is rapidly decelerated upon reaching the

standing water in the bay. It is suggested that sediment is transported in the accelerating flow as bedload and then suspended in the deeper bay water as the two water bodies meet. The suspended sediment is rapidly deposited as the flow stagnates. This process is identified due to the many observed cases in which there was a distinct transition from erosion to deposition upon the overwashing flow meeting the assumed maximum level of standing water on the back barrier during the storm.

In some cases, however, the transition from erosion to deposition occurred underwater, *i.e.*, landward of the peak bay water level. This always occurred where the foredune was narrower than in surrounding regions, or where the volume of sediment above the surge level was very small. It is suggested that this small subaerial volume was eroded during the storm and inundation overwash occurred. The coupling of ocean and bay water levels meant that flow deceleration caused by discharge into the bay was not sufficient to cause sediment deposition, indicating the importance of other processes subaqueously, such as friction or an adverse slope. This mechanism is illustrated in Figure 3-6.

Figure 3-7 shows the case where subaerial deposition of overwash occurs. Topography and friction act to decelerate subaerial overwash flow, and lateral spreading and infiltration act to reduce overwashing flow volumes. Either way, the sediment transporting capacity of the overwashing flow is reduced. Back barrier topography can either cause flow deceleration and sediment deposition due to adverse slopes, or may affect the back barrier flow by channelling overwash. In general the effect of overwash and washover deposition is to smooth the back barrier profile so the effect of adverse slopes may decrease as overwash progresses if the duration of overwash is sufficient. In **Paper V** it was suggested that overwashing flow tends towards a steady-state velocity determined by the balance between friction and gravity forces, where the friction force is proportional to the velocity squared. High observed velocities in subaerial overwash (**Paper VI**) therefore suggest significant friction forces acting on the overwash flow. If the initial overtopping velocity is faster than the steady-state velocity, friction will act to decelerate the flow. Vegetation, for example dune grasses, and established dune bushes may increase the amount of friction on the back barrier. Anthropogenic influences, for example roads and carparks may also affect the friction on the back barrier. The effect of roads and carparks on overwashing flow and washover deposition was seen to decrease for larger overwash flow depths (**Paper VI**), indicating that the effect of friction is also inversely dependent on the flow depth, as was suggested in **Paper V**.

Lateral spreading of confined overwash on the back barrier reduces the volume of flow parallel to the axis of the washover throat, hence reducing the transporting capacity of the overwashing flow in that direction. The result is reduced landward penetration of washover parallel to the flow axis, but increased volume of washover either side of this axis. Infiltration of overwashing flow into the back barrier also reduces the volume of flow and the transport capacity. Infiltration is dependent on the saturation of the back barrier, and is therefore more important at the start of an overwash event, and perhaps towards the end of the event if the timing of runup overwashes is such to allow drawdown of the back barrier water table between overwashing flows.

During unconfined inundation overwash the morphology change can generally be described as sediment removal from the foreshore, beach crest and front of the back barrier slope, with sediment deposition occurring towards the rear of the back barrier slope. In certain conditions, however, removal of sediment from the entire cross-shore barrier island occurs. Donnelly *et al.* (2006) described this as *barrier disintegration.* This was observed through the centre of section SR-A on Santa Rosa Island (**Paper VI**), where the island was narrowest. It is suggested that the cross-shore water level gradient is largest where the

island is narrowest, hence the more severe morphologic change observed. This mechanism is shown in Figure 3-8. Such conditions may proceed barrier breaching.

It is important to remember that the water level varies during overwash; hence the aforementioned processes may all be of importance at some stage during an overwash event. Also, a time-varying water level may cause the erosion of deposits made earlier during the same overwash event. Figure 3-9 suggests how the layering of washover deposits may develop under a receding water level where the only deposition mechanism is deposition at the standing water level. The period 1 deposits are deposited at the time of peak bay water level. At period 2, the bay water level has receded. Overwashing flow erodes the proximal end of the period 1 deposits, and deposits over the distal end and further downstream. Taking into account the time variation of washover deposit mechanisms is important for reconstructing storm history from the stratigraphic record (**Paper VI**).

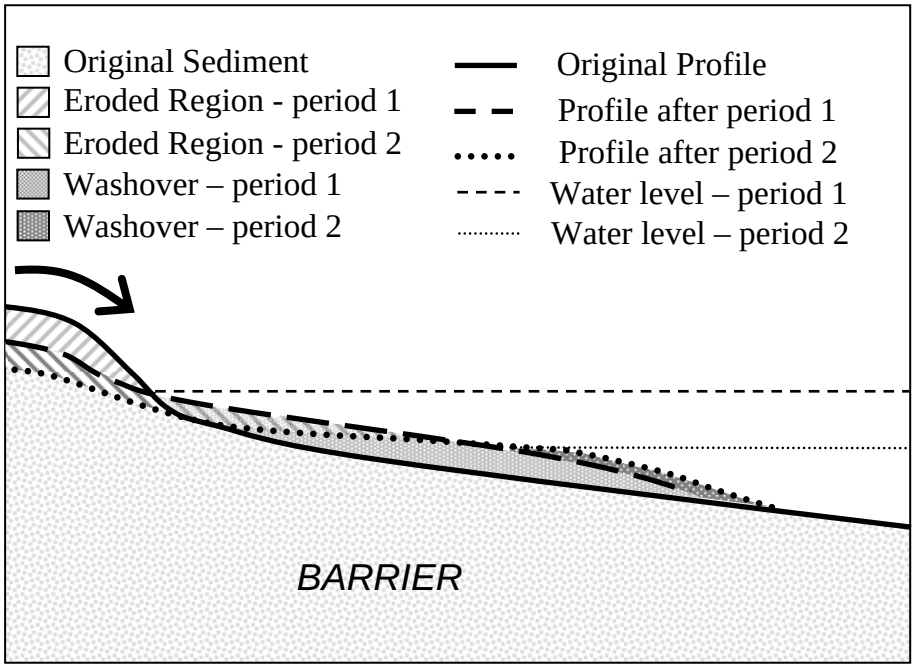

***Figure 3-9**. Schematic of back barrier region showing how time-varying water level affects subaqueous washover deposits. The barrier crest is on the left and flow is from left to right. Note the erosion of the proximal end of the period 1 deposit.*

4 Overwash Hydrodynamics

Quantifying the hydrodynamics of overwash on the beach crest and landward of the beach crest is necessary for understanding the processes which cause erosion and deposition during overwash and for quantifying water and sediment exchange from the ocean to the barrier and back barrier bay. Runup and inundation overwash hydrodynamics should be treated separately, due to the differences in flow regime at the beach crest and on the back barrier. The results from the laboratory experiments simulating runup overwash discussed in Chapter 2 are used to develop methods to predict runup overwash hydrodynamics on the beach crest and back barrier (**Paper V**). These results are further verified using published field measurements of overwash hydrodynamics (Fisher and Stauble 1977, Leatherman 1977, Holland et al. 1991, Matias 2006). Specifically, methods to estimate the overtopping wave height at the crest, the wave front velocity at the crest, and the development of the wave front velocity down the back slope are presented.

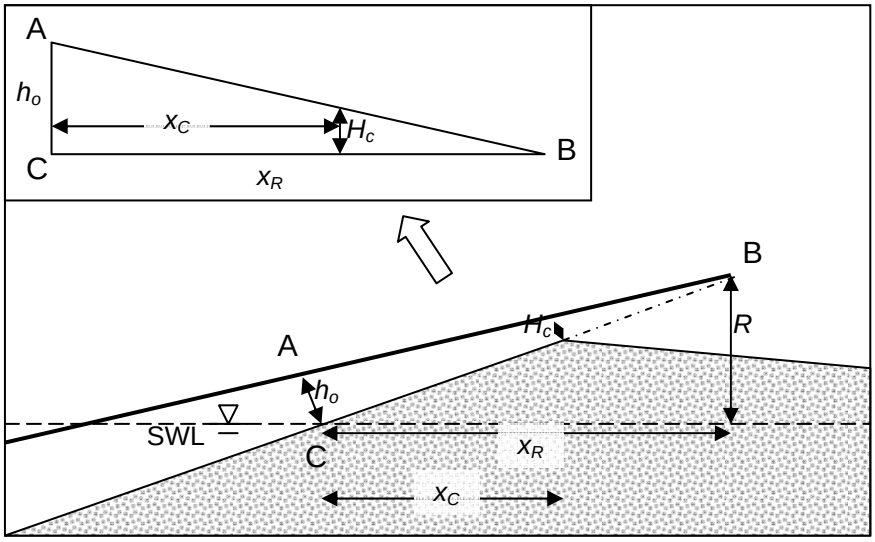

***Figure 4-1**. Sketch showing assumed water level at point of maximum runup, with inset of triangle ABC showing linear relationship used to estimate water depths (after Schuettrumpf and Oumeraci 2005).*

The maximum water depth at the crest during an overtopping wave, H_c, may be calculated from a similarity relationship, assuming a linear water profile at the time of maximum runup (Figure 4-1). This formulation is similar to that suggested by Schuettrumpf and Oumeraci (2005); however, it is expressed in terms of the water depth at the SWL during the time of maximum runup, h_o, rather than an empirical constant:

$$H_c = \frac{h_0}{x_R}(x_R - x_C) \quad \text{..... (4.1)}$$

where, x_R is the horizontal projection of maximum runup level, R, from the SWL calculated for known R using simple trigonometry, and x_c is the horizontal distance from the SWL to the beach crest.

A value of h_o was calibrated to best fit the data from the OWB3 experimental run, and the corresponding value for h_o/x_R (the calibration coefficient suggested by Schuettrumpf and

Oumerarci (2005) was then verified against the data from the OWB1 experimental run and field data. The calibrated value for h_o was then compared with a measured value of h_o extracted from the video data at a time of maximum water depth at the crest. The calibrated depth, 9.5 cm, compared well against the measured depths which ranged from 9 to 10 cm. The measured overtopping wave heights, H_c, from the experimental and field data are compared in Figure 4-2 to the values calculated using Eqn (4.1), where the horizontal projection of the runup height, x_R was calculated using the Hunt (1959) formula and the instantaneous beach slope was extracted from the video data. The results show good agreement for the laboratory data and a satisfactory agreement (within a factor of 3) for the field data, for which measurement accuracy was limited.

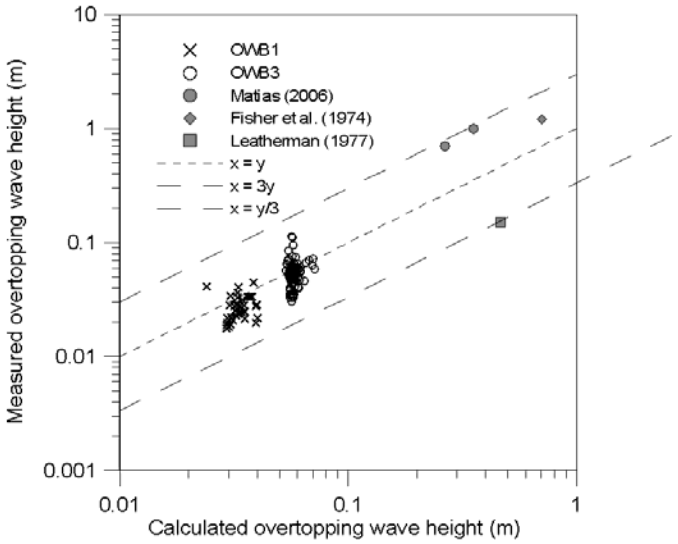

Figure 4-2. *Measured (laboratory and field) versus calculated overtopping wave heights*

The wave front velocity at the beach crest, u_{crest}, is calculated using a $\sqrt{gh}$ relationship. Figure 4-3 shows u_{crest} versus $\sqrt{gH_c}$ for the experimental runs (OWB1 and OWB3), and published field data, covering both laboratory and field scales as well as a wide range of forcing conditions. The linear regression relationship calculated at the crest is:

$$u_{crest} = 1.53\sqrt{gH_c} \quad \text{.....} \quad (4.2)$$

with an R^2 value of 0.79. This is very close to $u_{crest} = \sqrt{2gH_c}$ (also plotted in Figure 4-3), which may be derived for the velocity of gravity-driven flow exiting a tank of depth, H_c. This may be significant, as the crest represents a transition to gravity-influenced downhill flow.

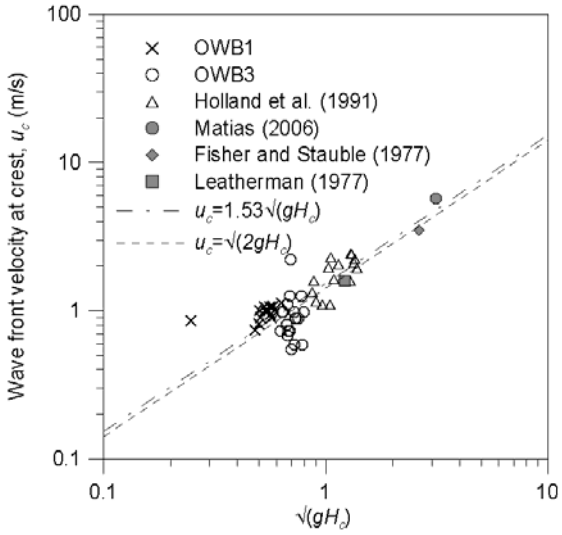

Figure 4-3. *Measured (laboratory and field) overwash front velocity at crest versus* $\sqrt{gH_c}$

On the back barrier, the evolution of the wave front velocity with distance may be calculated assuming the balance of friction and gravity forces on a small fluid element (ballistics theory), which represents the leading edge of the moving water. This is similar to how motion in the swash zone has been considered (without friction *e.g.* Shen and Meyer 1963, Ho *et al.* 1963, or with friction, *e.g.* Kirkgöz 1981, Hughes 1995) and assumes that the wave front is moving faster than the fluid behind it; hence the pressure acting on it is negligible (Ho *et al.* 1963). Here, friction is taken into account by assuming a shear stress proportional to the square of the velocity counteracting the flow. The equation of motion governing flow from the beach crest along a downward sloping planar back barrier is therefore:

$$\frac{du_B}{dt} = g\sin\beta_B - K_B u_B{}^2 \quad \text{.....(4.3)}$$

where u_B is the overwash front velocity, t is time, g is acceleration due to gravity, β_B is the slope of the back barrier, and K_B is a friction coefficient for the back barrier. Because the evolution of u_B down the back barrier is of interest, Eqn (4.3) is expressed in terms of the distance from the crest, down the back slope, s, using the relationship:

$$\frac{du_B}{dt} = \frac{ds}{dt}\frac{du_B}{ds} = u_B\frac{du_B}{ds} \quad \text{.....(4.4)}$$

which results in the following equation of motion down the back slope:

$$\frac{d\left(u_B^2\right)}{ds} = 2\left(g\sin\beta_B - K_B u_B^2\right) \quad \text{.....(4.5)}$$

This separable differential equation can be integrated and expressed in terms of u_B to give:

$$u_B(s) = \sqrt{\frac{g\sin\beta_B}{K_B}\left[1+\left(\frac{K_B u_0{}^2}{g\sin\beta_B}-1\right)e^{-2K_B s}\right]^{1/2}} \quad \text{.....(4.6)}$$

where u_o is an initial velocity at s = 0, usually at the beach crest. Hence, the variation in overwash wave front velocity down the back barrier slope may be calculated from the wave

front velocity at the beach crest and the distance traversed by the wave front. As the distance, *s*, approaches infinity, equation (4.6) can be shown to reach an asymptotic solution, or in other words, a steady-state velocity, given by:

$$u_B(\infty) = \sqrt{\frac{g \sin \beta_B}{K_B}} \quad \text{..... (4.7)}$$

Eqn (4.6) was tested on two different regions of flow on the back barrier during OWB3. The flow field for the OWB3 data is affected by the 'catch-up' of the 2nd harmonic wave at about s = 1 m. Seaward of this point, the decelerating trend relates to the first wave front and landward of this, the accelerating trend relates to the combined waves. The algorithm for flow on the back slope was therefore tested for these two regions separately, s = 0 to 1.1 m and s = 1.1 m to 5.5 m because the front speed would be the result of different initial conditions for the two regions. Figures 4-4 and 4-5 compare the measured and calculated overwash wave front velocities for OWB3. Note the differences in the steady state velocity and the optimum value of the friction coefficient, K_B, determined through a least squares fit. Given that there is an expected difference in depth between the two flow regions, a depth dependence of the friction coefficient, K_B might be expected. It is postulated that K_B is a function of the local wave height and that this formulation for evolution of the flow on the back barrier could be improved by taking the variation of the inverse of the local wave height, 1/ H_{ow}, in the direction of flow into account. Further experiments are suggested to verify this and to derive a suitable relationship for the friction coefficient on the back barrier in terms of $H_{ow}(s)$.

The three new formulations (Eqns 4.1, 4.2 and 4.6) present the ability to predict overtopping wave heights from the offshore wave forcing conditions, and hence the overwashing wave front velocity at the crest and on the back barrier.

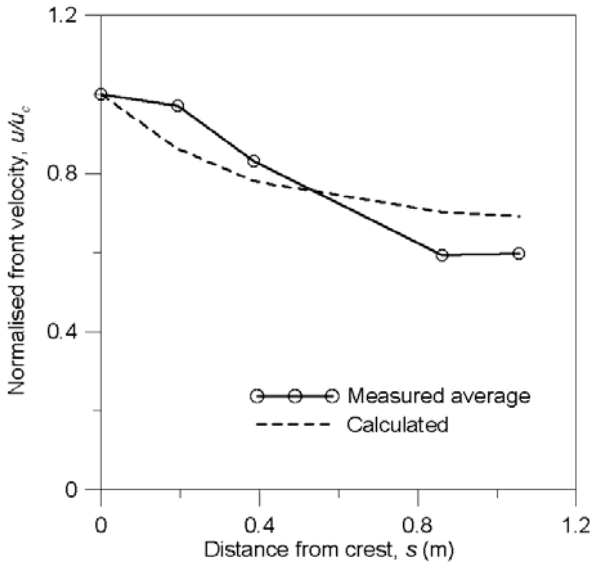

***Figure 4-4**. Measured and calculated average overwash wave front velocities, OWB3, s = 0 to 1.1 m, K_B = 0.76*

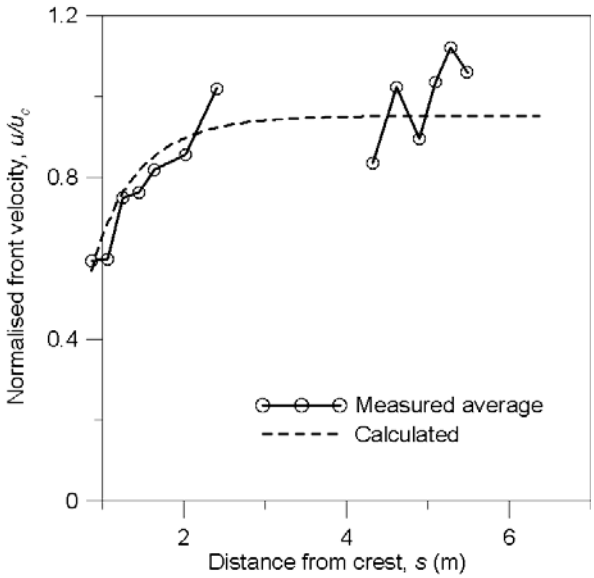

***Figure 4-5**. Measured and calculated average overwash wave front velocities, OWB3, s = 1.1 to 5.5 m, K_B = 1.7*

5 Predicting Beach Profile Change caused by Overwash

The ability to predict overwash occurrence, washover volumes and the cross-shore changes in beach profiles caused by overwash are emerging skills. The state of knowledge regarding overwash modelling is summarised in **Paper I**. Recent developments (including those since the publication of **Paper I**) in the ability to predict both the occurrence of overwash and the magnitude and shape of washover deposits are discussed here.

Sallenger (2000) used the relative elevations of the dune base and beach crest, and the peak surge and runup levels during an event to predict the occurrence of runup overwash, inundation overwash, and dune erosion. The approach is called a 'Storm Impact Scale' and was formulated with the intention of making regional scale, real-time predictions of overwash occurrence and severity (*runup overwash* versus *inundation overwash*, which are called overwash and inundation in the original article). Wetzell *et al.* (2003) used topographic lidar data from before and after Hurricane Dennis on a 17 km length of the Outer Banks, Northern Carolina, coastline to verify the method on a regional scale. Predictions of overwash occurrence generally coincided with overwash occurrence. One weakness in this approach is that the time-variation in beach crest elevations during a storm is not taken into account. Stockdon *et al.* (2007) applied the method to hindcast the effects of Hurricane Ivan on Santa Rosa Island, Florida. The alongshore accuracy of the impact predictions was 68 %. Stockdon *et al.* (2007) pointed out that in most locations where the predicted impact was incorrect, the impact was underestimated. This was attributed to the lack of predictability of the time-variation of the dune crest. For example, in regions with high dunes, overwash occurred after the dunes were eroded.

Jimenez et al. (2006) proposed the use of cumulative freeboad to predict washover volumes. Cumulative freeboard is the integral over time of the instantaneous freeboard, where freeboard is the difference between the runup level and the beach crest level. The uncertainty associated with using the pre-storm beach crest elevation to define freeboard was also analysed, by comparing this with the freeboard defined from the post-storm beach crest elevation. Because overwash may either increase or decrease beach crest heights, there may be either a positive or negative feedback to overwash occurrence over the course of a storm. Similarly, Nguyen et al. (2006) presented a new empirical formula to calculate washover volumes as a function of freeboard and storm duration, calibrating the model to new field data sets and verifying it against a further nine. Both models support the assumption that washover volume is a function of the freeboard and storm duration.

Tuan (2007) looked at the overwash on coastal barriers that leads to barrier breaching and constructed a numerical model to simulate this. In Tuan (2007) overwash is described as a process that lowers the barrier. In the context of the overwash processes discussed in Chapter 3, this is therefore overwash causing *barrier disintegration*. Subaerial deposition processes were not taken into account. A fixed bed and a moveable bed experiment were conducted, the first to study overtopping and the second to study detailed three-dimensional topographic change within a confined overwash flow. One objective of the study was to describe overtopping on an event basis rather than describing an average discharge rate. Such an approach is more useful and necessary for calculating the entrainment and transport of sediment. Tuan (2007) aimed to define the shape (time-variation) of an overtopping event on the crest as a function of time. This approach inspired the analysis of wave shapes presented in Chapter 4. Assuming a triangular distribution, Tuan (2007) introduced and quantified a wave-averaged overtopping time, a relative total overtopping

time, overtopping asymmetry, and the average instantaneous discharge – all at the beach crest. These parameters, however, were quantified from the time varying water depth at the crest, rather than from the time varying flow rate. Given that a time variation in depth averaged velocity is to be expected within each overtopping wave, the shapes of the time-varying water depth and time-varying flow rate are not the same. Also, in Chapter 4 it was shown that the defined parameters for the water depth vary with distance down the back slope. The novel approach by Tuan (2007), however, provides inspiration for further measurements and analysis. Tuan (2007) also used this description of the wave overtopping in a cross-island flow model based on the shallow water equations taking into account breach channel growth, including scour formation due to hydraulic jumps. The model was able to reproduce the barrier disintegration results seen in the moveable bed experiment. Note that all sediment was deposited subaqueously.

In this thesis, three different approaches to modelling beach profile change caused by overwash are presented. The approaches - parametric, analytic and numeric - represent varying degrees of complexity and computational accuracy, and hence, are suitable to a wide variety or applications. It was also intended to introduce simple process-based modelling which can account for a wide range of overwash forcing and back barrier processes using readily available input data.

5.1 Parametric Approach

It is useful to be able to qualitatively predict the occurrence of different types of profile response to an overwash event through some simple, empirically-based criterion using readily available data on the storm and beach profile conditions. Such predictions are useful for schematically determining the severity of an overwash event or for determining how the barrier evolves, for example, in long-term barrier evolution modelling.

In **Paper II** the incipient profile morphology and overwash forcing conditions are used to qualitatively predict the expected morphology response type, using the morphology response type categories proposed by Donnelly *et al.* (2006) and summarised in Section 3. More than 50 sets of pre- and post-storm profile data with the associated wave height, wave period, and water level time-series were assembled and used to test a variety of dimensionless parameters to estimate the overall response of a profile to an overwash event. The associated hydrodynamic forcing data was only available for a few profiles showing response types 5, 6 or 7, so these were grouped into the 'barrier response' category. For each category, the number of profiles with available hydrodynamic forcing is listed in Table 5-1. It is important to note that barrier response type is not entirely defined by the pre-storm morphology, hence the need to relate it to the forcing. For example, a low flat barrier without a prominent dune may still undergo crest accumulation or landward translation of the beach crest.

Table 5-1: Distribution of profile data among cross-shore profile change types following overwash

Cross-shore profile change type	Number of profiles
1. Crest Accumulation	9
2. Landward Translation of Dunes/Berms (Dune Translation)	7
3. Dune Lowering	8
4. Dune Destruction	22
5. Barrier Response (Barrier Accretion and Barrier Overwash)	9

Readily available, objectively definable morphologic and hydrodynamic parameters thought to affect the resulting washover deposits were selected. The morphologic parameters, defined by the pre-storm profile, found to be of importance were the beach or dune (hereafter referred to as beach) crest level above mean sea level, z_D, the foreshore slope, s_{ave}, dune front and rear slopes, s_f and s_r, where $s = \tan \beta$, the dune height, D, and the width of the top of the dune, B_D. Additionally, a representative dune volume, V_D, was calculated according to

$$V_D = \frac{1}{2} D^2 \left(\frac{1}{s_f} + \frac{1}{s_r} \right) + B_D D \quad \text{..... (5.1)}$$

This dune volume, per unit dune length, approximates the relative amount of material available in the dune for overwash. This value is zero where dunes do not exist. Barrier width was also thought to be of importance, but data were not available. This is because most survey data is collect for the purpose of monitoring beaches and shorelines rather than monitoring entire barrier systems, which would be necessary for overwash.

The hydrodynamic parameters available and deemed to be important were the maximum significant deepwater wave height occurring during the event, H_0, the peak wave period corresponding to that height, T, the maximum surge level (including tide) occurring during the event, S, and overwash duration, t_s. Runup levels, R, were calculated after Wise *et al.* (1996), using H_0, T and s_{ave}, where R is the runup excursion if the slope, s_{ave}, extends indefinitely. Using R, the overwash duration, t_s, was defined as the duration where the total water level $R + S$ exceeded the initial dune crest level, z_D. Additionally, a new parameter, F, taking into account both the magnitude and duration of overtopping, was calculated by integrating the excess runup level, $R + S - z_D$, over the overwash duration, t_s, according to Jimenez *et al.* (2007).

Dimensional analysis was used to determine non-dimensional parameters from the aforementioned parameters. Such analysis yields many combinations of parameters, so only those which made physical sense were selected for testing. Each morphology response type category was assigned a different symbol for plotting, and two-dimensional plots of the non-dimensional parameter values were made. If there is some relation between the plotted parameters and the profile response, some regional separation of one or more of the response types will be seen. Where the region was able to be delineated, a criterion was defined. Figure 5-2 shows the results of various non-dimensionless parameter plots revealing information for each of the morphology response types.

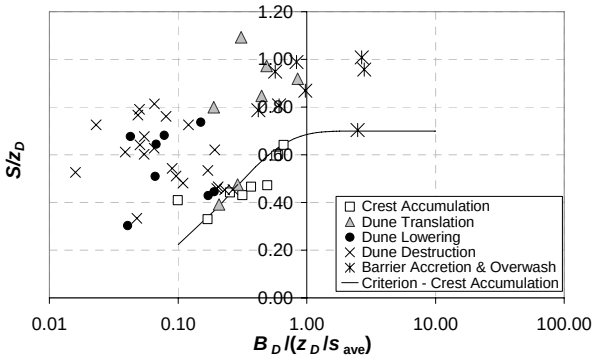

(a) S/z_D vs $B_D/(z_D/s_{ave})$ – Crest Accumulation

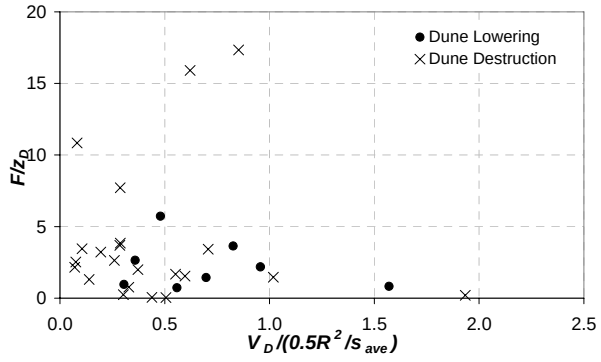

(b) F/z_D vs $V_D/(0.5R^2/s_{ave})$ – Dune Responses

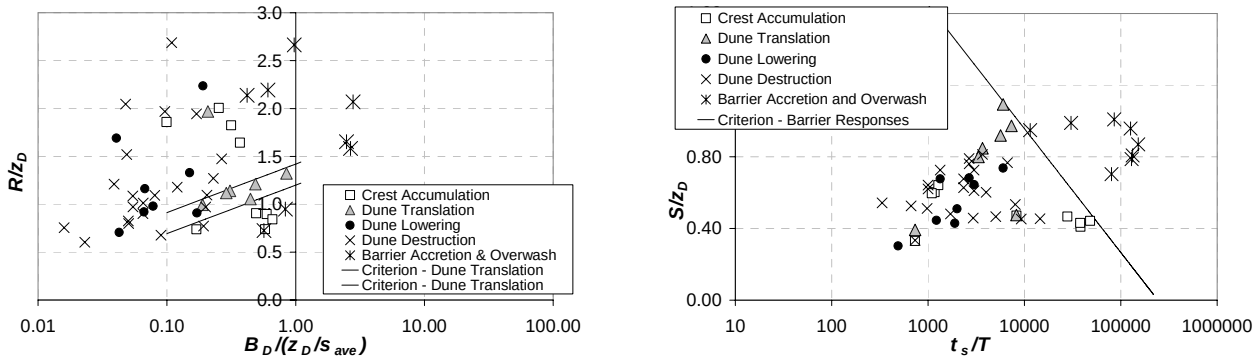

(c) R/z_D vs $B_D/(z_D/s_{ave})$ – Dune Translation

(d) S/z_D vs t_s/T – Barrier Accretion and Overwash

***Figure 5-2**. Non-dimensional parameter plots showing delineation of different morphology response types.*

The results indicate that crest accumulation overwash is controlled by surge level and beach crest width (Figure 5-2a). Contrary to expectation, variations in runup level did not determine this response type (*e.g.* Figure 5-2c). Some reasons for this are proposed in **Paper II**. The dune response types, dune translation and lowering were both restricted to narrow crest widths, *i.e.* the existence of a dune, but also to higher surge and runup levels than crest accumulation (Figures 5-2a and 5-2c). The two response types could not be separated by storm duration, as expected; however, there is some indication that larger dune volumes limit the occurrence of dune destruction (Figure 5-2b). The barrier overwash response types were controlled by surge level and storm duration (Figure 5-2d). The results also indicated to some extent that dune translation is limited to a small range of runup levels and dune widths (Figure 5-2c); however, the processes causing this can only be inferred.

The approach was successful in delineating some of the morphology response types, and hence identifying the hydrodynamic and morphologic parameters controlling the morphology response. Crest accumulation, a combined category of dune lowering and destruction (dune response types), and the barrier response types could be clearly separated from each other using the simple non-dimensional parameters. There is also some indication that the landward translation of dunes and berms response type may be delineated in this way. The defined criterion may therefore be used to predict overwash response morphologies using readily available storm forecast data and existing profile cross-sections.

5.2 Analytical Approach

Simple efficient methods to calculate the response of schematised profiles to storms are useful for predicting order-of-magnitude profile response, for example washover volumes and contour retreat, using limited input data. An analytical model predicting the subaerial beach response to dune erosion caused by wave impact and overwash was developed and validated using high-quality field data (**Paper III**). The model calculates the eroded volume, overwash volume, beach crest reduction, and contour-line retreat for a schematised barrier island subject to wave impact and overwash. Such results are useful as inputs to long-term barrier modelling, or, for example, for calculating empirical risk functions for the occurrence of different storm impacts.

A barrier island was represented by a simple schematised triangular profile. It was therefore definable by three points: 1. the crest height, z_D, 2. the seaward (front) beach foot location at the SWL, x_o, and 3. the shoreward (rear) beach foot location at the SWL, x_B, as defined in

Figure 5-3. Many of the barrier profiles analysed by Donnelly *et al.* (2006) and in **Paper II** have simple triangular shapes. Overwash is determined to occur depending on the relative elevations of the theoretical wave runup level, water level and beach crest level. If the beach crest height is exceeded by the water level, the runup level is not defined and inundation is assumed to occur. The theoretical wave runup level is the runup level of the wave if the seaward slope of the beach had continued infinitely upwards. If overwash occurs, a portion of the sediment mobilised by wave impact is defined as being transported landward and the rest is transported seaward. Otherwise all the sediment mobilised is transported seaward.

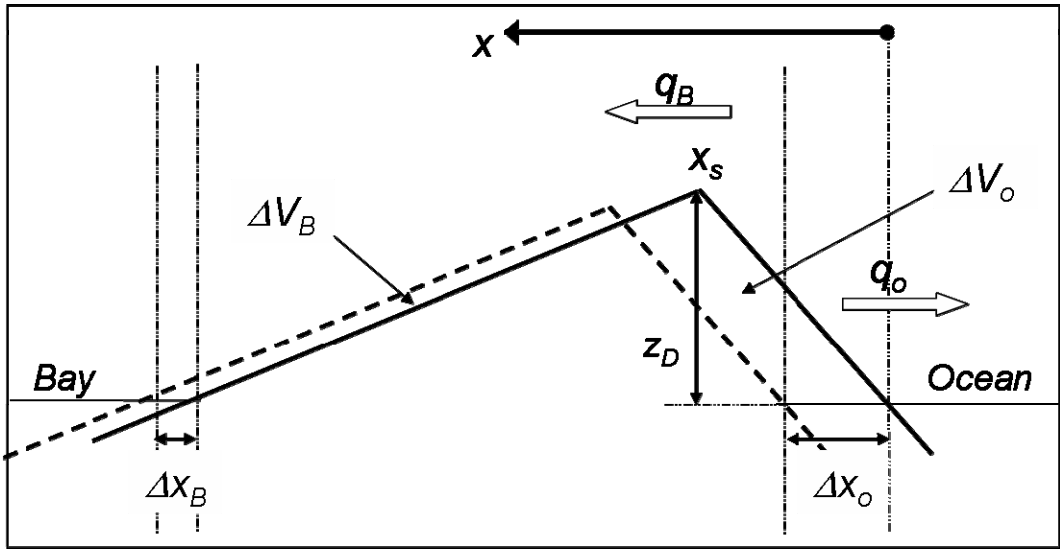

***Figure 5-3**. Schematic of a beach cross-section subject to wave impact and overwash. The dotted profile is the profile after overwash occurrence.*

It was assumed that a volume of sediment, ΔV_o, is mobilised by wave impact over a period of time, Δt. If overwash occurs, a portion of this mobilised sediment volume, ΔV_B, is deposited subaerially on the back barrier as overwash, while the rest, ΔV_o - ΔV_B, is eroded offshore. Using the conservation equations for sediment volume, analytical equations to calculate the time evolution of the triangular beach were derived for known q_B, and q_o, the sediment transport rates over the beach crest (landward), and offshore (seaward), respectively.

The subaerial volume of the dune, V_D, is calculated from the dune geometry:

$$V_D = \frac{1}{2}(x_B - x_o)z_D \quad \text{.....} (5.2)$$

Also from the dune geometry, the overwashed and seaward volumes of sediment after time Δt are: $\Delta V_B = \Delta x_B\, z_D$ and $\Delta V_o = \Delta x_o\, z_D$, respectively, assuming small changes. At the limit where Δt approaches zero, the sediment eroded from the ocean side of the profile, ΔV_o, may be expressed in terms of the seaward and landward sediment transport rates, q_o and q_B, respectively, using the sediment conservation relationship:

$$\frac{dV_o}{dt} = (q_o + q_B) \quad \text{.....} (5.3)$$

Similarly, the overwashed volume deposited landward of the beach crest, ΔV_B, is expressed by:

$$\frac{dV_B}{dt} = q_B \quad \text{.....(5.4)}$$

Changes in the subaerial dune volume, V_D, are only caused by offshore loss of material, q_o. Sediment transported landward, q_B, is retained by the barrier island; hence, the rate of change of barrier island volume is expressed as a function of q_o only:

$$\frac{dV_D}{dt} = -q_o \quad \text{.....(5.5)}$$

Assuming q_o is constant over time and an initial beach volume of V_{Do} at $t = 0$, Eqn (5.5) is solved to give:

$$V_D = V_{Do} - q_o t \quad \text{.....(5.6)}$$

This is more conveniently expressed in terms of x_B and x_o, using the geometric relationships shown above, and where $\Delta V_D = \Delta V_B - \Delta V_o$:

$$\frac{d(x_B - x_o)}{dt} = -\frac{q_o}{z_D} \quad \text{.....(5.7)}$$

An expression for z_D may be obtained in terms of the initial dune volume and dune geometry using Eqns (5.2) and (5.6):

$$z_D = 2\frac{V_{Do} - q_o t}{x_B - x_o} \quad \text{.....(5.8)}$$

The time evolution of (x_B - x_o) may now be solved for by substituting this expression for z_D into Eqn (5.7) and solving the differential equation yielding:

$$x_B - x_o = l_{Do}\sqrt{1 - \frac{q_o t}{V_{Do}}} \quad \text{.....(5.9)}$$

where $l_{Do} = x_{Bo}$-x_{oo}. Since we are interested in the time evolution of the beach crest height, z_D, Eqn (5.8) can again be used to express Eqn (5.9) in terms of z_D, yielding the final expression for the time evolution of the beach crest height:

$$z_D = z_{Do}\sqrt{1 - \frac{q_o t}{V_{Do}}} \quad \text{.....(5.10)}$$

where z_{Do} is the beach crest height at $t = 0$ and is equal to $2V_{Do}/l_{Do}$.

It is also of interest to derive the time evolution of x_o and x_B. Using the volume relationships, $\Delta V_o = \Delta x_o z_D$ and $\Delta V_B = \Delta x_B z_D$ substituted into Eqns (5.3) and (5.4) respectively, the following two relationships for x_o and x_B result:

$$\frac{dx_o}{dt} = \frac{q_o + q_B}{z_D} \quad \text{.....(5.11)}$$

$$\frac{dx_B}{dt} = \frac{q_B}{z_D} \quad \text{.....(5.12)}$$

Solving these equations, the beach crest height, z_D, may be replaced with the relationship derived in Eqn (5.10), yielding the final expressions for the time evolution of x_o and x_B:

$$x_o = x_{oo} + l_{Do}\left(1+\frac{q_B}{q_o}\right)\left(1-\sqrt{1-\frac{q_o t}{V_{Do}}}\right) \quad \text{.....(5.13)}$$

$$x_B = x_{Bo} + l_{Do}\frac{q_B}{q_o}\left(1-\sqrt{1-\frac{q_o t}{V_{Do}}}\right) \quad \text{.....(5.14)}$$

Eqns (5.10), (5.13) and (5.14) therefore describe the time evolution of the triangular shaped beach in terms of the initial geometry of the beach, x_{oo}, x_{Bo}, l_{Do} and V_{Do}, and in terms of the seaward and landward sediment transport rates, q_o and q_B, respectively.

An empirical relationship relating the ratio q_B/q_o to the relative elevations of the beach crest height and runup level was derived. It was inferred that as the maximum elevation of theoretical runup increases in relation to the beach crest height, the quantity of sediment transported as overwash increases. **Paper III** describes a database of overwashed beach profile measurements with associated wave, and water level data covering five different storms and four different locations. The total change in barrier volume, V_D and overwash volume, V_B was calculated from each profile set and the eroded volume from the seaward side of the beach, V_o, calculated according to $V_o = V_D + V_B$. The average transport rates, q_o and q_B, were then calculated by dividing the measured volumes with a duration of overwash inferred from the water level and wave data.

The ratio q_o/q_B for each beach profile data set was then plotted against the ratio between the initial beach crest height z_{Do}, and the peak theoretical runup level for the storm, R, as seen in Figure 5-4. Both the best linear fit and non-linear fit are plotted with the data; however, q_o/q_B should approach infinity as z_{Do}/R approaches one because no overwash occurs. The non-linear fit was therefore used to derive the following empirical equation:

$$\frac{q_o}{q_B} = A\frac{z_{Do}/R}{1-z_{Do}/R} \quad \text{.....(5.15)}$$

where A is an empirical constant with a value of 3.

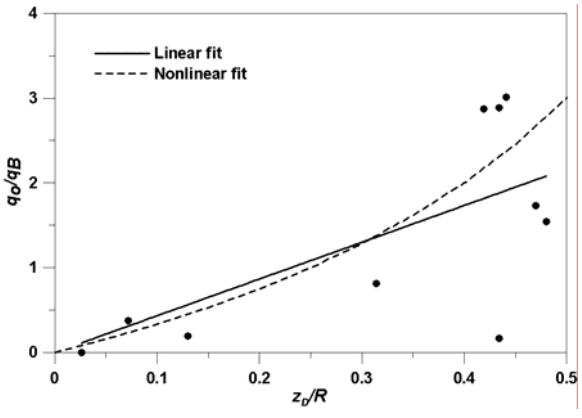

Figure 5-4. Ratio between average offshore (q_o) and overwash (q_B) transport as a function of relative ratio between initial beach crest height and maximum theoretical runup level, z_{Do}/R.

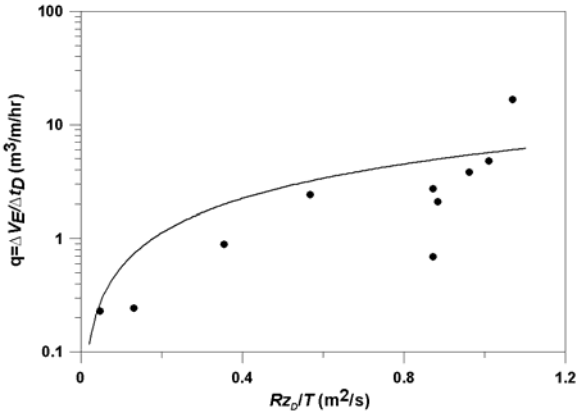

Figure 5-5. Eroded volume, q, during storms where overwash occurred, as a function of the modified impact parameter, Rz_D/T

The relationship $q = q_o + q_B$ can then be used to calculate q_o and q_B if q is known. One of the governing assumptions of this analytical approach is that sediment is mobilised by wave impact. Larson *et al.* (2004a) developed a sediment transport formula for the sediment eroded from a dune face due to wave impact. The formula derives from work by Fisher *et al.* (1986), and is based on the assumption that the weight of sediment eroded from the dune is linearly proportional to the force on the dune due to the change in momentum flux of bores impacting on the dune (impact). For the simple case where the runup height, R, and the dune foot elevation, z_o, are constant, this is expressed as:

$$V = V_o - 4C_s(R - z_o)^2 \frac{t}{T} \quad \text{.....(5.16)}$$

where V is the volume eroded from the dune, V_o is the initial dune volume, C_s is an empirical transport coefficient, z_o is the vertical distance between the water level and the dune foot, and t / T is the number of waves impacting the dune for a storm duration, t and wave period, T. In the case of overwash, the theoretical runup level exceeds the beach crest, *i.e.* $R - z_o > z_D$, so it is thought that the wave impact might be reduced compared to the case where the entire wave impacts the beach. A correction factor taking this into account, $z_D / (R - z_o)$ is therefore applied to Eqn (5.16), yielding:

$$q = \frac{dV}{dt} = -4C_s \frac{(R - z_o)^2}{T} \frac{z_D}{R - z_o} = -4C_s \frac{(R - z_o)}{T} z_D \quad \text{.....(5.17)}$$

Using the aforementioned data set, the value of q was calculated by dividing the measured change in volume with the duration of overwash inferred from the water level and wave data. Figure 5-5 shows the observed values of q as a function of the modified impact parameter, and a linear fit to the data according to Eqn (5.17). The best fit line corresponds to a C_s value of 4.10^{-4}, which is similar to values obtained by Larson et al (2004a).

Ideally, a number of volume and shape measurements in time would be used to validate the derived algorithms; however, profile measurements during an overwash event are rare due to the obvious dangers associated with collecting such data during a severe storm or hurricane. Additionally, only initial profile geometry and peak storm surge parameters were used since introducing variation in the water level and wave characteristics would also require using the time variation of the morphology, and hence, a numerical approach. Since the objective here is a simple analytical approach, such limitations are reasonable.

The results of validating the algorithms against field data sets indicate that the model captures the overall volumetric response of subaerial profile. In particular, Figures 5-4 and 5-5 indicate that the trends between total volume changes and storm forcing and between onshore/offshore deposition ratio and excess runup level are well represented and that this approach may provide order-of–magnitude estimates of the main morphological parameters. The complete study, including a more thorough derivation of the impact model and applications of the theory, is published in **Paper III**.

5.3 Numerical Approach

The ability to predict the location and thickness of washover deposits is of importance for coastal residents, coastal town planners, environmental scientists, and engineers, among others. For coastal engineers, robust predictions of beach profile changes caused by overwash may be useful in designing nourished beach profiles, protective coastal sand dunes, and other soft engineering structures. Coastal residents and the engineers who plan coastal settlements might be interested in locating infrastructure behind the line of predicted

washover intrusions. Geologists might be interested in the washover penetration of historical storms as marsh-building platforms, and ecologists may be interested in available washover habitat created. There exists, therefore, a need for a robust model, employing readily available data, to calculate beach profile changes caused by overwash. As mentioned in Section 5.2, the desire to model the time-varying water level and wave characteristics in tandem with the time-variation of the beach profile requires a numerical approach.

Paper IV introduced a new numerical model that simulates the sediment transport and 2D beach and back barrier profile change caused by overwash. The model was formulated to be as general as possible, taking into account a wide variety of incipient beach profiles, representing, for example, the presence and absence of dunes, and both overwash regimes. It is based on physical descriptions of the governing processes, but simplifies these to some extent, in order to employ readily available data, and retain the generality and robustness of the model. On the back barrier, overwash is an unsteady, shallow flow affected by lateral spreading, friction, infiltration, and uneven topography. The state-of-the-art of unsteady flow modelling makes the representation of these processes and their interactions very difficult; hence, the average flow on the back barrier is approximated as a block of water at steady-state, taking into account lateral spreading, friction and infiltration. **Paper V** showed that overwash wave front velocities trend towards a steady-state velocity, which was suggested to be defined by the balance between friction and gravitational forces. The sediment transport rate at the beach crest is calculated according to one of two different algorithms, taking into account the overwash regime, runup or inundation overwash. To calculate the forcing at the surf zone boundary, these algorithms were then implemented within a numerical model for beach profile change during storms, SBEACH (Larson and Kraus 1989), validated and verified against a large data set of pre- and post-storm beach profiles where overwash had occurred.

An overwashed beach was divided into three separate regions for consideration, the swash zone, the beach crest, and the back barrier. Here the algorithms derived for overwash over the beach crest and back barrier are described. During runup overwash, the overtopping rate (the volumetric rate of water passing the beach crest) may be calculated from the velocity and water depth at the crest according to continuity. A velocity at the crest, u_{crest}, may be calculated from ballistics theory in the same way as ballistics theory is often applied to swash front velocities (*e.g.*, Shen and Meyer 1963):

$$u_{crest} = \sqrt{2g(R - z_D)} \quad (5.18)$$

where g is acceleration due to gravity, z_D is the vertical position of the beach crest relative to the still water level and R is the theoretical runup level, *i.e.*, the runup level of the waves, had the beach slope extended indefinitely.

The duration of overtopping, t_D, is also derived from ballistics theory, assuming a swash period corresponding with the wave period, T.:

$$\frac{t_D}{T} = \sqrt{1 - \frac{z_D}{R}} \quad (5.19)$$

where T is the wave period. Assuming the front of the uprushing wave behaves like a bore, the water depth, h_D, can be derived from a simple bore front equation $ucrest = C_U \sqrt{gh_D}$ where C_U is a bore front coefficient. In **Paper V**, this assumption was shown to be reasonable. The overtopping rate is then simply derived as the water depth, h_D, multiplied by u_D from Eqn (5.18). Here, we are interested in the average volume of flow per

overtopping wave, $\dot{V}_{DR}$, which is obtained by multiplying the overtopping rate by the relative duration, t_D/T, obtained in Eqn (5.19):

$$\dot{V}_{DR} = \frac{2\sqrt{2g}}{C_U^2}(R - z_D)^{3/2}\sqrt{1 - \frac{z_D}{R}} \quad \text{.....(5.20)}$$

For inundation overwash, it was proposed that the elevation of the water level relative to the beach crest is the most important factor affecting the flow rate, *i.e.*, the gravity driven flow of the excess water level over the beach crest dominates the wave processes. This is consistent with the conclusions of Pirrello (1992). The ocean side of the crest is assumed to act as a large reservoir, and the beach crest as a weir, with flow accelerating over the crest onto the back barrier. The overtopping flow rate, $\dot{V}_{DI}$, is therefore described using the weir equation:

$$\dot{V}_{DI} = \frac{2}{3}C_d\sqrt{2gh_D^3} \quad \text{.....(5.21)}$$

where C_d is a weir coefficient and h_D is the excess water level over the crest, taken to be S-z_D, where S is the surge level. Note that the transition to inundation overwash is taken to occur when the surge level, not including wave setup, exceeds the beach crest. Some inundation may occur when the surge level including wave setup inundates the crest; however, it is estimated that wave overtopping would still dominate sediment transport at this water level.

For both runup and inundation overwash, the overwashing sediment rate was assumed proportional to the flow rate. Hancock and Kobayashi (1994) and Kobayashi *et al.* (1996) presented measurements of overtopping rates and sediment concentrations over a variety of overwash magnitudes showing this relationship. This is therefore a convenient and, at the same time, reasonable approximation. Assuming a constant concentration of sediment in the overtopping flow, the following equations for overwash transport over the crest were obtained for runup overwash, q_{DR}, and inundation overwash, q_{DI}, respectively:

$$q_{DR} = 2K_B\sqrt{2g}(R - z_D)^{3/2}\sqrt{1 - \frac{z_D}{R}} \quad \text{.....(5.22)}$$

$$q_{DI} = 2K_B\sqrt{2gh_D^3} \quad \text{.....(5.23)}$$

Note that the same coefficient, K_B, is used to take into account both the sediment concentration and the bore properties for the case of runup overwash, and the sediment concentration and the weir coefficient for the case of inundation overwash. If Eqns (5.20) and (5.21) are equated for the limiting inundation case, *i.e.* runup overwash occurring for a duration $t/T = 1$, and assuming that h_D corresponds to R-z_D, it can be seen that the formulations for q_{DR} and q_{DI} are mathematically equivalent, and the following relationship for the coefficients arises:

$$C_u = \sqrt{\frac{3}{C_d}} \quad \text{.....(5.24)}$$

In **Paper V**, a value of approximately 1.53 was derived for C_u, yielding a C_d value of around 1.3, which is a realistic value for a weir coefficient. This suggests that K_B is a suitable coefficient taking into account both bore front and weir processes for the two regimes, the introduction of which is a convenient formulation making the overwash model easy to apply.

On the back barrier, a single algorithm is used to describe the hydrodynamics and sediment transport of both runup and inundation overwash flow landward of the beach crest. Flow on the back barrier is thought to be controlled by the balance between friction and gravitational forces, and, thus, to trend towards a steady flow state. The distance from the crest to where this steady flow state is reached, is assumed to be short; hence, the flow is assumed to be steady and described by a block of water moving down a slope. This schematised block is depicted in Figure 5-6. As the block moves down the back barrier slope, which is assumed to be constant, the flow disperses due to lateral spreading, and gets shallower due to infiltration. The assumption of a constant slope is a simplification; however, the results for profiles with secondary dunes shown in **Paper IV** suggest that they may still be represented in this way. In **Paper VI**, it was shown that the back barrier profile changes towards a constant slope during overwash; hence the constant slope represents conditions at some stage during an event.

The continuity equation for this block, assuming that infiltration is proportional to the height of the block, *h*, is given by:

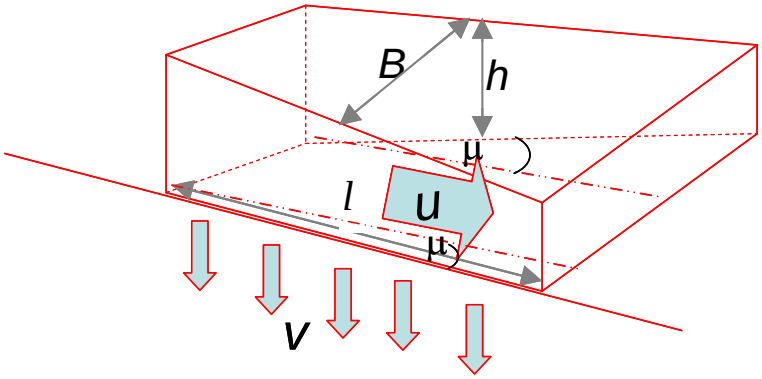

***Figure 5-6**. Schematic of a block of water moving down slope with lateral spreading and infiltration.*

$$\frac{dV}{dt} + \alpha hBl = \frac{dV}{dt} + \alpha V = 0 \quad \text{.....(5.25)}$$

where $V = Bhl$ is the volume of water in the block, α is the proportionality constant for infiltration, and B and l are the width and length of the block, respectively. Solving this equation for V, and dividing by the flow velocity yields the following expression for the flow depth:

$$h = \frac{B_D}{B} h_D e^{-\alpha t} \quad \text{.....(5.26)}$$

where B_D and h_D are the width and height of the block at the beach crest respectively. The length of the block, l, is assumed constant. Eqn (5.26) yields h as a function of time; however, h may be expressed in terms of the distance travelled by the block from the beach crest, s, using $t = s/u$, where u is derived from the balance of friction and gravity forces on the block:

$$u = k_f \sqrt{gh} \quad \text{.....(5.27)}$$

where for a back barrier slope of β,

$$k_f = \sqrt{\frac{2\sin\beta}{f_c}} \quad \text{.....(5.28)}$$

The evolution of the water depth, *h*, along the back barrier slope becomes then an implicit equation for *h*:

$$h = \frac{B_D}{B} h_D e^{-\alpha s/u} = \frac{B_D}{B} h_D e^{-\frac{\alpha}{k_f}\frac{s}{\sqrt{gh}}} \quad \text{.....(5.29)}$$

A linear spreading rate, μ, is then used to estimate the width of flow, *B*, at distance, *s*, down the back barrier slope according to:

$$B = B_D\left(1+\mu\frac{s}{B_D}\right) \quad \text{.....(5.30)}$$

This is then substituted into Eqn (5.29) yielding the final expression for the evolution of the flow depth on the back barrier slope:

$$h = \frac{1}{1+\mu s/B_D} h_D e^{-\frac{\alpha}{k_f}\frac{s}{\sqrt{gh}}} \quad \text{.....(5.31)}$$

Paper IV furthermore explains how these algorithms are implemented within a numerical model for simulating storm-induced beach change. Eqn (5.31) was made non-dimensional by replacing the water depth, *h*, with *u*, in order to calculate the sediment transport on the back barrier assuming a transport rate proportional to the velocity cubed. The boundary conditions at the seaward end of the swash zone are required as input to the swash algorithm presented in **Paper IV**, and therefore to the derived overwash algorithms. Additionally, some kind of a model updating changes to the subaqueous portion of the beach is required to ensure a realistic feedback between the subaqueous and subaerial beach hydrodynamics. The SBEACH model (Larson and Kraus 1989, Wise et al. 1996) was chosen for this purpose; although it is pointed out that any similar beach profile change model could have been used. A finite difference scheme was used to solve the sediment continuity equation for each time-step after the transport rates had been calculated.

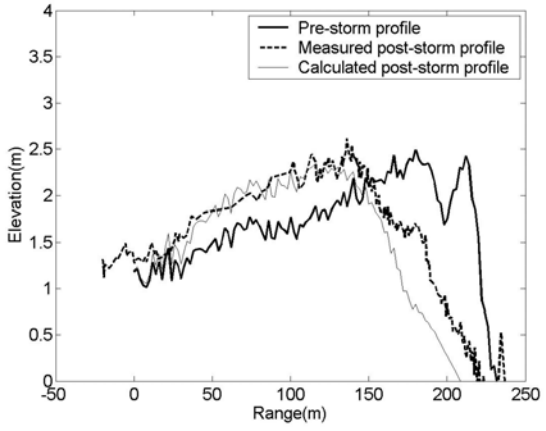

Figure 5-7a *– Results of model calibration for profile 3720 at Assateague Island, MD*

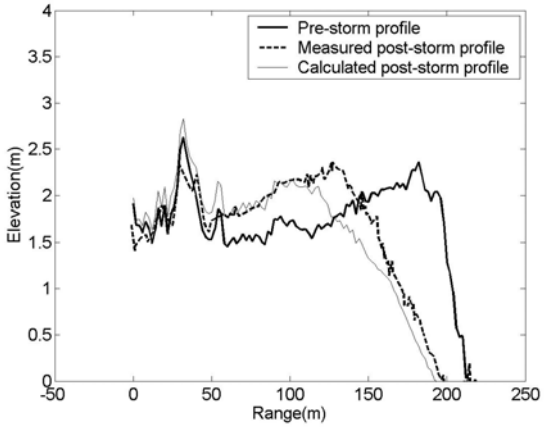

Figure 5-7b *– Results of model verification for profile 2330 at Assateague Island, MD*

Figure 5-7 shows an example of model calibration and verification results at Assateague Island, Maryland. The model was applied to the field data sets using default values of non-overwash calibration parameters present in SBEACH (*e.g.* Wise *et al.* 1996). Three

parameters affecting overwash were varied. These were the crest overwash parameter, K_B, a lateral spreading parameter, $C_{ls} = \mu/B_D$ and infiltration parameter, $C_{infilt} = \alpha/u_D$. The throat width at the crest, B_D, is included within C_{ls}, because such data is usually unavailable with beach profile data, and including u_D provides a convenient non-dimensional form of the sediment transport. These parameters were varied for the calibrated profile and then the same parameters used to verify the model performance on other profiles. It was possible to achieve a good calibration and verification result for a wide range of beach profile types and overwash magnitudes, including both runup and inundation overwash. The calibrated values for the various regions are listed in **Paper IV**.

The algorithm was also tested using more detailed inputs, making the model more generalised, such that the calibrated model is applicable to a wider range of cross-shore profiles. Donnelly and Sallenger (2007) presented new topographic data of overwash fans on Hatteras Island, North Carolina. This 3-D data, allowed the possibility to input actual washover throat widths and lateral spreading angles, in order to produce a more generalised cross-shore overwash profile change model. Beach profiles were taken through the centre of a washover throat. The calibration coefficients expressed above were reformulated such that the initial washover throat width, B_D, and a potential lateral spreading angle, μ, could be entered. For simplicity, infiltration was assumed to be negligible. The K_B coefficient remains in the algorithm to represent the proportion of sediment in the overtopping flow along with a bore front/weir coefficient for the runup overwash/inundation overwash modules, respectively.

Initial washover throat widths were measured from an alongshore section of the dune ridge crest. It is acknowledged that the throat width varies during overwash, but in a predictive mode, the pre-storm throat width is specified. This value was kept constant during the simulation. Potential lateral spreading angles were then identified using the pre-storm topography confinement. In a predictive mode, lateral spreading angles may be derived, where possible, using pre-storm topography confinement, but note that anthropogenic influences and vegetation affect lateral spreading significantly. Where a previous fan exists, the lateral spreading angle of the old fan may provide a good initial estimate. In the absence of a better estimate, an angle of 30 degrees represents the average lateral spreading angle of the fans measured by Donnelly and Sallenger (2007). An example of the model calibration and verification results using initial throat widths and lateral spreading angles as inputs is shown in Figure 5-8. Again, it was possible to achieve a good calibration and the verification was deemed satisfactory, recreating the dune erosion and redistribution of dune sediments on the back slope reasonably well.

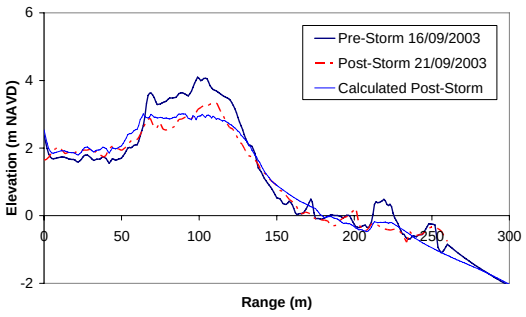

***Figure 5-8a**. Results of model calibration for Fan C, Hatteras Island, North Carolina.*

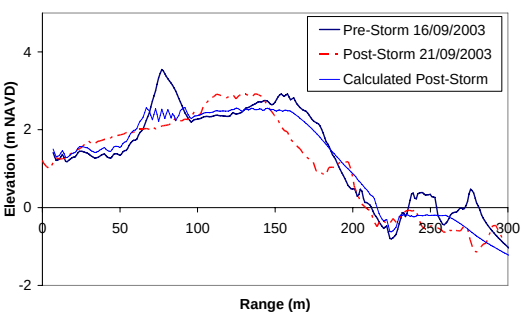

***Figure 5-8b**. Results of model verification for Fan B, Hatteras Island, North Carolina.*

6 Conclusions

In this thesis, new understanding of overwash processes with respect to both the forcing and shaping mechanisms, and new methods to predict overwash hydrodynamics and beach profile change caused by overwash, are presented. A state-of-knowledge on measuring and modelling of overwash and overwash processes was compiled from previously published overwash studies. Summarising all previous work on overwash allowed for the processes to be inferred, and the data requirements and scope for future work to be clearly defined. As a result, a large new data set of pre- and post-storm beach profile change caused by overwash, along with the associated hydrodynamic forcing data, was compiled from the open literature and from city, state, and consulting engineers, and beach protection authorities. Also, new mid-scale experiments of runup overwash on a low flat barrier island and a barrier with a prominent dune were conducted, for which hydrodynamics on profile change on the beach crest and back barrier were a focus.

These new data sets inspired the categorisation of washover morphology into seven different morphology response types, which were then linked to the incipient morphology and forcing conditions. This not only introduce the ability to predict the qualitative profile change caused by overwash, but it also increases the understanding of the forcing processes which determine washover magnitude and form. The laboratory data set was analysed to determine the hydrodynamics of runup overwash on the back slope and to develop algorithms to predict the hydrodynamics at the beach crest from the forcing data and the associated evolution of the hydrodynamics along the back barrier slope. Qualitative and quantitative observations from the laboratory experiments also enhanced the understanding of overwash processes.

Analytic and numerical models of beach profile change due to overwash were developed according to state-of-the-art understanding of overwash processes, and calibrated and verified against the new data sets. The analytical model results indicated that the model captures the overall response of the subaerial profile and may provide order-of-magnitude estimates of main morphological parameters. The numerical model is capable of reproducing a wide range of overwash morphologies including dune crest erosion, dune destruction, barrier rollback, the thinning of a washover deposit on the backbarrier, and overwash over a multiple dune system, and can be used in a predictive mode when calibrated and verified using the calibrated coefficients for a similar location.

There remains scope to further develop the ability to predict beach profile change caused by overwash. Specifically, the understanding of overwash processes presented here stimulates new requirements for hydrodynamic overwash data. Runup overwash flow on the back barrier is a pulsing, unsteady flow, so measurements of Eulerian velocities at the beach crest and on the back barrier are therefore required to develop more detailed physical relationships for the spatial and time variation of flow rates, depths and velocities from which sediment transport may be calculated. In **Paper V**, the friction forces were shown to be inversely proportional to the flow depth. Further measurements are required to determine this relationship. Inundation overwash hydrodynamics have been described according to the relative elevations of the ocean and bay water levels and the beach crest. Measurements are required to validate and further develop these descriptions. **Paper VI** shows that flow deceleration in a standing water body is an important process. Similar processes that may provide inspiration for modelling this process include river delta formation or landslide flows into water bodies. Theory to qualitatively describe this process is lacking for the discharge of both steady and unsteady flows into standing water, *i.e.* inundation and runup overwash, hence there is scope for further study on this.

The overall aim of this project was to improve the capability to predict sediment transport by overwash and, hence, topographic changes caused by overwash. It is believed that the new knowledge regarding overwash processes and hydrodynamics, and three different methods to predict beach profile changes caused by overwash presented here provide a needed step in that direction.

7 References

Baldock, T.E., Hughes, M.G., Day, K., and Louys, J. 2004. Swash overtopping and sediment overwash on a truncated beach. *Coastal Engineering*, 52, 633-645.

Bradbury, A. P. and Powell, K. A. 1992. The short term profile response of shingle spits to storm wave action. *Proceedings 23rd Coastal Engineering Conference*, ASCE, 2694-2707.

Byrnes, M. R. and Gingerich K. J. Cross-island profile response to Hurricane Gloria. *Proceedings Coastal Sediments '87* (ASCE), New Orleans, 1987. Kraus N.C., ASCE, New York, 1486-1502.

Canny, J.F. 1986. A computational approach to edge detection. *IEEE Trans. Pattern Analysis and Machine Intelligence*, 679-698.

Carter, R. W. G. and Orford, J. D. 1981. Overwash processes along a gravel beach in South-East Ireland. *Earth Surface Processes and Landforms*, 6(5), 413-426.

Chen, Q., Wang, L., and Tawes, R. (Submitted). Hydrodynamic response of northeastern Gulf of Mexico to hurricanes. Submitted to Journal of Geophysical Research.

Dillon, W.P. 1970. Submergence effects on a Rhode Island barrier lagoon and inferences on migration of barriers. *Journal of Geology*, 78, 94-106.

Dolan, R. and Godfrey, P. 1973. Effects of Hurricane Ginger on the barrier islands of North Carolina. *Geological Society of America Bulletin*, 84, 1329-1334.

Donnelly, C., Wamsley, T.V., Kraus, N.C., Larson, M., and Hanson, H. 2006. Morphologic classification of coastal overwash. *Proceedings 30th Coastal Engineering Conference*, ASCE, 2805-2817.

Donnelly, C. and Sallenger, A. H. Jnr. 2007. Characterisation and modelling of washover fans. *Proceedings Coastal Sediments '07*, ASCE, 2061-2073.

Edge, B.L., Park, Y.H., and Overton, M. 2007. Experimental study of overwash. *Proceedings Coastal Sediments* '07, ASCE, 2074- 2083.

Erikson, L. and Hanson, H. 2005. A method to obtain wave tank data using video imagery and how it compares to conventional data collection techniques, *Journal of Computers and Geosciences*, 31, 371-384.

Fisher J. S., Leatherman, S. P., and Perry, Capt. F. C. 1974. Overwash processes on Assateague Island. *Proceedings 14th Coastal Engineering Conference*, ASCE, 1194-1211.

Fisher, J. S. and Stauble, D. K. 1977. Impact of Hurricane Belle on Assateague Island washover. *Geology*, 5, 765-768.

Fisher, J.S., Overton, M.F., and Chisholm, T. 1986. Field measurements of dune erosion. *Proceedings 20th Coastal Engineering Conference*, 1986, ASCE, 1107-1115.

Godfrey, P. J., and Godfrey, M. M. 1974. The role of overwash and inlet dynamics in the formation of salt marshes on North Carolina barrier islands, in: Reinold, R. A. (Ed.), *Ecology of Halophytes*. New York Academic Press, 407-427.

Hancock, M., and Kobayashi, N. 1994. Wave overtopping and sediment transport over dunes. *Proceedings 24th Coastal Engineering Conference*, ASCE, 2028-2042.

Hancock, M. W. 1994. Experiments on irregular wave overtopping and overwash of dunes. MSc Thesis, Department of Civil Engineering, University of Delaware, U.S.A., 88 pp.

Ho, D.V., Meyer, R.E., and Shen, M.C. 1963. Long surf. *Journal of Marine Research*, 21, 219-230.

Holland, T. K., Holman, R. A., and Sallenger, A. H. Jnr. 1991. Estimation of overwash bore velocities using video techniques. *Proceedings Coastal Sediments '91*, ASCE, 489-497

Hughes, M.G. 1995. Friction factors for wave uprush. *Journal of Coastal Research*, 11,

1089-1098.
Hughes, M.G. and Baldock, T.E. 2004. Eulerian flow velocities in the swash zone: Field data and model predictions. *Journal of Geophysical Research*, 109.
Hunt, I.A., 1959. Design of seawalls and breakwaters. *Journal of the Waterways and Harbors Division*, ASCE 85 (WW3), pp 123-152.
Jimenez, J.A., Sallenger, A.H., and Fauver, L. 2006. Sediment transport and barrier island changes during massive overwash events. *Proceedings 30th Conference of Coastal Engineering*, ASCE, 2870-2879.
Kirkgoz, M.S., 1981. A theoretical study of plunging breakers and their runup. *Coastal Engineering*, 5, 353-370.
Kobayashi, N., Tega, Y., and Hancock, M.W. 1996. Wave reflection and overwash of dunes. *Journal of Waterway, Port, Coastal and Ocean Engineering*, 122, 150-153.
Kraft, J. C., Biggs, R. B., and Halsey, S.D. 1973. Morphology and vertical sedimentary sequence models in Holocene transgressive barrier systems, in: Coates, D. R., (Ed.), *Coastal Geomorphology*: Publications in Geomorphology, State University of New York, 321-354.
Kraus, N.C. 2006. Understanding piping plover population dynamics through mathematical model, with application to northern Assateague Island, Maryland, and Long Island, New York, Barrier beaches. *Shore and Beach*, 74, 3-9.
Larson, M. and Kraus, N.C. 1989. SBEACH. Numerical Model for Simulating Storm-induced Beach Change; Report 1. Empirical Foundation and Model Development. *Technical Report CERC-89-9*, U.S. Army Engineer Waterways Experiment Station, Coastal Engineering Research Center, Vicksburg, MS, 267 pp.
Larson M., Wise R. A., and Kraus N. C. 2004. Modeling dune response due to overwash transport. *Proceedings 29th Coastal Engineering Conference*, ASCE, 2133-2145.
Larson, M., Erikson, L., and Hanson, H. An analytical model to predict dune erosion due to wave impact. *Coastal Engineering*, 2004, 59(8/9), 675-696.
Leadon, M.E., 1999. Beach, dune and offshore profile response to a severe storm event. *Proceedings Coastal Sediments '99*, ASCE, 2534-2549.
Leatherman, S. P. 1976. Quantification of overwash processes, Ph.D. Dissertation, Department of Environmental Sciences, University of Virginia, Charlottesville, VA, 245 pp.
Mansard, E.P.D. and Funke, E.R. 1980 The Measurement of Incident and Reflected Spectra Using a Least Squares Method, *Proceedings 17th Conference of Coastal Engineering*, ASCE 154-172.
Matias, A. 2006. Overwash sedimentary dynamics in the Ria Formosa barrier islands. PhD Thesis, U. Algarve, Portugal, 253 p. Available at: http://www.ualg.pt/ciacomar/downloads/PhD-Matias-2006.pdf
Morton, R. A. 1979. Subaerial storm deposits formed on barrier flats by wind-driven currents, *Sedimentary Geology*, 24, 105-122.
Morton, R. A. and Sallenger A. H., Jr. 2003. Morphological impacts of extreme storms on sandy beaches and barriers. *Journal of Coastal Research*,19, 560-573.
Nguyen, X.T., Donnelly, C., and Larson, M. 2006. A new empirical formula for coastal overwash volume. *Proceedings Vietnam-Japan Estuary Workshop*, Water Resources University, Vietnam, 60-65.
Parchure, T., Dean, R. G., and Srinivas, R. 1991. Laboratory study of overwash on barrier islands. Progress Report, Coastal and Ocean Engineering Department, University of Florida, U.S.A., 59 pp.
Pirrello, M. A. 1992. The role of wave and current forcing in the process of barrier island overwash. MSc. Thesis, Coastal and Ocean Engineering Department, University of Florida, 117pp.

Sallenger, A.H. Jr. 2000. Storm impact scale for barrier islands. *Journal of Coastal Research*, 16(3), 890-895.

Sallenger Jr., A. H., Krabill, W. B., Swift, R. N., Brock, J., List, J., Hansen, M., Holman, R. A., Manizade, S., Sontag, J., Meredith, A., Morgan, K., Yunkel, J. K., Frederick, E. B., and Stockdon, H. 2003. Evaluation of airborne topographic lidar for quantifying beach changes. *Journal of Coastal Research*, 19, 125-133.

Schuettrumpf, H. and Oumeraci, H. 2005. Layer thicknesses and velocities of wave overtopping flow at seadikes. *Coastal Engineering*, 52, pp 473-495.

Schwartz, R. K. 1978. Nature and genesis of some storm washover deposits. *Technical Memorandum TM-61*, U.S. Army Engineer Research Center, Coastal Engineering Research Center, Fort Belvoir, Virginia.

Shen, M.C. and Meyer, R.E. 1963. Climb of a bore on a beach: Part three Run-up. *Journal of Fluid Mechanics*, 16, 113-125.

Srinivas, R., Dean R.G., and Parchure, T.M. 1992. Barrier island erosion and overwash study – Vol. 1. Coastal and Ocean Engineering Department, University of Florida, U.S.A, 92pp.

Stockdon, H. F., Thompson, D M., and Sallenger, A.H. 2007. Hindcasting potential hurricane impacts on rapidly changing barrier islands. *Proceedings Coastal Sediments '07*, ASCE, 976-985.

Stone, G.W., Liu, B., Pepper, D.A., and Wang, P. 2004. The importance of extratropical and tropical cyclones on the short-term evolution of barrier islands along the northern Gulf of Mexico, USA. *Marine Geology*, 210, 63-78.

Tuan, T.Q. 2007. Seasonal breaching of coastal barriers. PhD Thesis, Department of Coastal Engineering, Delft University, The Netherlands, 177pp.

Wang, P. and Horwitz, M.H.. 2006. Erosional and depositional characteristics of regional overwash deposits caused by multiple hurricanes. *Sedimentology*, 1-20.

Weir, G.M. 1977. Inlet formation and washover processes at North Pond, eastern Lake Ontario. Masters Thesis. University of New York at Buffalo. Buffalo NY, 75 pp.

Wetzell, L. M., Howd, P. A., and Sallenger, A. H. 2003. Simple models for predicting dune erosion hazards along the Outer Banks of North Carolina. *Proceedings Coastal Sediments '03*, CD-ROM Published by World Scientific Press and East Meets West Productions, Corpus Christi, TX ISBN-981-238-422-7, 10 pp.

Williams, P.J. 1978. Laboratory development of a predictive relationship for washover volume on barrier island coastlines. MSc Thesis, Department of Civil Engineering, University of Delaware, U.S.A., 141 pp.

Wise, R. A., Smith, S.J., and Larson, M. 1996. SBEACH: Numerical model for simulating storm-induced beach change. Report 4. Cross-shore transport under random waves and model validation with SUPERTANK and field data, *Technical Report CERC-89-9*, U.S. Army Engineer Waterways Experiment Station, Coastal Engineering Research Center, Vicksburg, MS.

.